Circadian rhythms of macrophages are altered by the acidic pH of the tumor microenvironment.

Amelia M. Knudsen-Clark[1], Daniel Mwangi[2], Juliana Cazarin[2], Kristina Morris[2], Cameron Baker[3], Lauren M. Hablitz[4], Matthew N. McCall[2,5,6], Minsoo Kim[1,6], Brian J. Altman[2,6,*].

[1]Department of Microbiology and Immunology, [2]Department of Biomedical Genetics, [3]Genomics Research Center, [4]Center for Translational Neuromedicine, [5]Department of Biostatistics and Computational Biology, and [6]Wilmot Cancer Institute, University of Rochester Medical Center, Rochester, New York, USA.

*Corresponding author.

E-mail: Brian_Altman@URMC.rochester.edu

Abstract

Macrophages are prime therapeutic targets due to their pro-tumorigenic and immunosuppressive functions in tumors, but the varying efficacy of therapeutic approaches targeting macrophages highlights our incomplete understanding of how the tumor microenvironment (TME) can influence regulation of macrophages. The circadian clock is a key internal regulator of macrophage function, but how circadian rhythms of macrophages may be influenced by the tumor microenvironment remains unknown. We found that conditions associated with the TME such as polarizing stimuli, acidic pH, and elevated lactate concentrations can each alter circadian rhythms in macrophages. Circadian rhythms were enhanced in pro-resolution macrophages but suppressed in pro-inflammatory macrophages, and acidic pH had divergent effects on circadian rhythms depending on macrophage phenotype. While cyclic AMP (cAMP) has been reported to play a role in macrophage response to acidic pH, our results indicate that pH-driven

changes in circadian rhythms are not mediated solely by the cAMP signaling pathway. Remarkably, clock correlation distance analysis of tumor-associated macrophages (TAMs) revealed evidence of circadian disorder in TAMs. This is the first report providing evidence that circadian rhythms of macrophages are altered within the TME. Our data further suggest that heterogeneity in circadian rhythms at the population level may underlie this circadian disorder. Finally, we sought to determine how circadian regulation of macrophages impacts tumorigenesis, and found that tumor growth was suppressed when macrophages had a functional circadian clock. Our work demonstrates a novel mechanism by which the tumor microenvironment can influence macrophage biology through altering circadian rhythms, and the contribution of circadian rhythms in macrophages to suppressing tumor growth.

Introduction

Tumor-associated macrophages (TAMs) are one of the most abundant leukocytes found in solid tumors, with high intra-tumoral TAM density generally associated with poor clinical outcome [1-3]. This is consistent with the largely pro-tumorigenic role of macrophages within tumors[4]. Macrophages are highly plastic professional phagocytes whose ability to sense and respond to the environment makes them uniquely equipped to protect tissue integrity under normal homeostatic conditions[5, 6]. However, within the chronically inflamed tumor microenvironment (TME), failure to resolve the inflammation can lead to uncontrolled secretion of tissue repair factors by TAMs, promoting tumor growth and metastatic capacity[7-9]. At the same time, conditions in the TME can drive TAMs to suppress potentially anti-tumorigenic inflammatory activity through various mechanisms including secretion of anti-inflammatory cytokines and expression of checkpoint inhibitors such as PD-L1, promoting immune suppression[4, 10-16].

TAMs are known to suppress the response to many standard of care treatments through their pro-tumorigenic and immunosuppressive functions, making them a prime therapeutic target[17]. However, we still have an incomplete understanding of how the TME influences macrophages, limiting our ability to target them; this is highlighted by the varying efficacy of therapeutic approaches used to target macrophages[18]. This is thought to be due in part to the significant phenotypic heterogeneity of TAMs within tumors[18-20]. Evidence suggests this heterogeneity is due to the ability of macrophages to sense and adapt to the local microenvironment, which varies within tumors depending on several factors including the distance from blood vessels and neighboring cells[21-24]. Indeed, various conditions in the TME have been shown to influence macrophage phenotype and function[4].

In particular, poor vascularization of solid tumors leads to inefficient delivery of oxygen, creating regions of hypoxia[25]. The hypoxic response promotes enhanced glycolytic activity of cells within the region, which, coupled with poor tissue drainage as a result of leaky vasculature, results in elevated levels of protons and lactate, acidifying the microenvironment[26, 27]. Of conditions in the TME, it has been well appreciated that acidic (low) pH can promote a pro-resolution phenotype, thereby contributing to the pro-tumorigenic and immunosuppressive functions of macrophages within tumors[28-30].

The myriad ways in which the TME can impact regulation of macrophages remain to be fully elucidated. Circadian rhythms are a key regulatory system present in almost all cells of the body, and are an understudied facet of macrophage biology[31]. Acidic pH is a condition commonly associated with the TME that has been shown to alter circadian rhythms in cell lines[32]; however, whether pH influences circadian rhythms in macrophages remain unknown.

Circadian rhythms are 24-hour rhythms that impart oscillations in the levels of circadian-regulated gene transcripts and proteins in a tissue- and cell-specific manner, resulting in time-of-day-dependent variation in many cellular processes[33, 34]. The molecular clock, which we will refer to as the circadian clock, drives these rhythms in cells through a cell-autonomous transcription/translation feedback loop, which is controlled in part by the transcription factor BMAL1[31]. Circadian clocks are synchronized by signals sent out from the central circadian clock housed within the suprachiasmatic nucleus of the hypothalamus, which entrains circadian clocks to the time of day[31]. This allows for the temporal coordination of cells in spatially distinct tissues, although how the local microenvironment influences circadian rhythms remains to be elucidated.

All leukocytes tested to date have functional circadian clocks[35-42]. As such, nearly every arm of the immune response (both innate and adaptive) is subject to circadian regulation[35, 37, 43]. Time-of-day-dependent regulation of immune responses is achieved though temporal gating of response to stimuli, effector function, and cell trafficking[42, 44-48], all of which promote coordination between the multiple phases of the immune response[40, 42, 49-53].

Key aspects of macrophage function are subject to circadian regulation, including cytokine secretion and phagocytosis[36, 44, 45, 51, 54]. This results in a time-of-day-dependent macrophage response to stimuli, which modulates the magnitude of the resulting adaptive immune response and determines disease progression[44, 51, 55]. Circadian regulation of macrophages is of particular interest given recent evidence of 24-hour circadian variation in the frequency of TAMs expressing surface markers associated with pro- or anti-tumorigenic phenotypes[56-58]. A promising application of such circadian variation was made evident in leveraging observations of circadian frequency in TAMs expressing immune checkpoint blockade (ICB) target PD-1 to increase efficacy of PD-1/PD-L1 ICB therapy by timing treatment to the time of day when PD-1+ TAMs were most frequent[57, 59]. This suggests that leveraging time-of-day variations in therapeutic targets could be a promising avenue to increase efficacy, highlighting the importance of understanding how circadian rhythms of macrophages may be influenced by conditions in the TME, which remains unclear.

In this work, we present evidence that circadian rhythms of macrophages are altered in the TME. We uncover a novel way in which two conditions within the TME, acidic pH and lactate, can influence macrophage biology through modulation of circadian rhythms. We also find that macrophages of different phenotypes have distinct circadian rhythms. Remarkably, we found evidence of circadian disorder in tumor-associated macrophages, indicating that circadian rhythms are altered in macrophages

within the TME. Furthermore, our data suggest that heterogeneity in circadian rhythms at the population level may underlie the observed circadian disorder. This work elucidates a novel way in which the TME can alter macrophage biology, and represents the first steps to understanding how the tumor microenvironment can alter circadian rhythms of immune cells such as macrophages.

Results

Macrophages of different phenotypes exhibit different circadian rhythms.

As macrophages are a phenotypically heterogeneous population in the TME, we first sought to understand whether diversity in macrophage phenotype could translate to diversity in circadian rhythms of macrophages. To this end, we used two well-established *in vitro* polarization models to study distinct macrophage phenotypes[5, 60-63]. For a model of pro-inflammatory macrophages, we stimulated macrophages with interferon gamma (IFNγ) and lipopolysaccharide (LPS) to elicit a pro-inflammatory phenotype[60, 64]. These macrophages are often referred to as 'M1' and are broadly viewed as anti-tumorigenic, and we will refer to them throughout this paper as pro-inflammatory macrophages[65, 66]. For a model at the opposite end of the phenotypic spectrum, we stimulated macrophages with IL-4 and IL-13[60, 67]. While these type 2 stimuli play a role in the response to parasites and allergy, they are also major drivers of wound healing; in line with this, IL-4 and IL-13-stimulated macrophages have been well-characterized to adopt gene expression profiles associated with wound-healing and anti-inflammatory macrophage phenotypes[68-71]. As such, these macrophages are often used as a model to study pro-tumorigenic macrophages *in vitro* and are often referred to as 'M2' macrophages; throughout this paper, we will refer to IL-4 and IL-13-stimulated macrophages as pro-resolution macrophages[66, 72, 73]. Consistent with previous studies, we found that genes associated with anti-inflammatory and pro-

resolution programming characteristic of IL-4 and IL-13-stimulated macrophages such as *Arg1, Retnla, Chil3* (Ym1), *Clec10a* (MGL1)*, and Mrc1 (*CD206*)* were induced in IL-4 and IL-13-stimulated macrophages, but not IFNγ and LPS-stimulated macrophages. In contrast, genes associated with pro-inflammatory activity characteristic of IFNγ and LPS-stimulated macrophages such as *Nos2* (iNOS)*, Tnfa, Il1b, and Il6* were induced in IFNγ and LPS-stimulated macrophages, but not IL-4 and IL-13-stimulated macrophages (Supplementary Figure 1)[28, 30, 65, 71, 74, 75]. This indicates that macrophages stimulated with IL-4 and IL-13 were polarized toward a pro-resolution phenotype, while macrophages stimulated with IFNγ and LPS were polarized toward a pro-inflammatory phenotype.

Circadian rhythms of macrophages were measured by monitoring PER2, a key component of the circadian clock, via the rhythmic activity of the PER2-Luciferase (PER2-Luc) fusion protein in a live cell LumiCycle luminometer (Supplementary Figure 2A)[76]. Bone marrow-derived macrophages (BMDMs) were generated from bone marrow of mice expressing PER2-Luc. Following differentiation, the circadian clocks of BMDMs were synchronized by a 24-hour period of serum starvation followed by 2 hours of serum shock[77], and rhythms were observed for up to 4 days (Supplementary Figure 2B,C).

To determine whether phenotype can influence circadian rhythms in macrophages, BMDMs were cultured in the presence or absence of polarizing stimuli, and rhythms were observed by LumiCycle (Figure 1). The amplitude of rhythms is the magnitude of change between the peak and the trough, and is indicative of the strength of rhythms[78, 79]. Amplitude of rhythms was suppressed in pro-inflammatory macrophages compared to unstimulated macrophages. In contrast, amplitude of rhythms in pro-resolution macrophages was enhanced. This suggests that rhythms are suppressed in pro-inflammatory macrophages but enhanced in pro-resolution macrophages, which agrees with previous observations[80, 81]. Period is the amount of time it takes to complete one full oscillation[82].

Compared to unstimulated macrophages, period was lengthened in pro-resolution macrophages but shortened in pro-inflammatory macrophages. This In line with others' observations and suggests that the clock runs with a longer period (slower) in pro-resolution macrophages but runs with a shorter period (faster) in pro-inflammatory macrophages[80, 81].

Interestingly, we observed differences in damping of rhythms in polarized macrophages. Damping is measured as the number of days required for the amplitude of rhythms to decrease by 30% of the first cycle[83]. Damping of rhythms in most free-running cell populations (defined as cells cultured in the absence of external synchronizing stimuli) occurs naturally as the circadian clocks of individual cells in the population become desynchronized from each other; thus, damping can be indicative of desynchrony within a population[84]. The damping rate increases as the time it takes for rhythms to dissipate decreases; conversely, as damping rate decreases as the time it takes for rhythms to dissipate increases. We observed increased rate of damping in pro-inflammatory macrophages compared to unstimulated macrophages (Figure 1), indicating that population-level rhythms were maintained for a shorter length of time in pro-inflammatory macrophages. In contrast, damping rate was decreased in pro-resolution macrophages, indicating that population-level rhythms were maintained for longer in pro-resolution macrophages. These data suggest that pro-inflammatory macrophages may have an impaired ability to maintain synchrony, while pro-resolution macrophages may have an enhanced ability to maintain synchrony.

Collectively, these data suggest that pro-inflammatory macrophages have weaker rhythms and impaired ability to maintain synchrony, while pro-resolution macrophages have enhanced rhythms and an increased ability to maintain synchrony. This is evidence that macrophages of different phenotypes have

176 distinct circadian rhythms, suggesting that diversity of macrophage phenotype may lead to diversity in
177 macrophage circadian rhythms.
178
179 **Acidic pH alters circadian rhythms of macrophages.**
180
181 The TME has previously been shown to be acidic, with a pH ranging from 6.8 to 6.3; much more acidic
182 than the typical pH in blood and healthy tissue of 7.3-7.4[85-87]. It was previously reported that acidic
183 pH can alter circadian rhythms, but whether this applies to macrophages remains unknown[32]. Thus,
184 we cultured BMDMs under conditions of varying pH within a range that mimics that found within the
185 TME (pH6.5-pH7.4). As macrophages are a heterogeneous population in the TME, we assessed the
186 influence of acidic pH on rhythms of unstimulated, pro-resolution, and pro-inflammatory macrophages.
187 In line with previous observations, macrophages cultured at pH 6.5 were polarized toward a pro-
188 resolution phenotype, characterized by increased expression of *Arg1* and *Vegf* compared to
189 macrophages cultured at pH 7.4 (Supplementary Figure 3A). Pro-inflammatory macrophages cultured at
190 pH 6.5 had decreased expression of *Nos2* compared to those cultured at pH 7.4, suggesting that an
191 acidic pH of 6.5 both promotes a pro-resolution phenotype and suppresses a pro-inflammatory
192 phenotype.
193
194 It has been observed that inducible cyclic AMP early repressor (*Icer*), an isoform of cyclic AMP (cAMP)-
195 response modulator (*Crem*), is upregulated downstream of acid-sensing in macrophages, and has been
196 used as a “biomarker” for macrophages exposed to acidic conditions in tumors. We observed induction
197 of *Icer* in unstimulated and pro-resolution macrophages cultured at pH 6.5 compared to pH 7.4,
198 indicating that these macrophages were sensing acidic conditions (Supplementary Figure 3B). In line with
199 previous observations that *Icer* is induced downstream of LPS-driven TLR4 signaling, *Icer* was also

upregulated in pro-inflammatory macrophages compared to unstimulated macrophages even at neutral pH 7.4[88]. Although *Icer* was not further upregulated in pro-inflammatory macrophages at pH 6.5 compared to pH 7.4, *Nos2* was suppressed at pH 6.5 compared to pH 7.4, suggesting that pro-inflammatory macrophages responded to acidic pH. In all, these data confirm that macrophages of various phenotypes can sense and respond to acidic conditions within the range of pH found in the TME.

To determine whether an acidic microenvironment can influence circadian rhythms in macrophages, we assessed rhythms of unstimulated, pro-resolution, and pro-inflammatory macrophages under normal and acidic conditions. To this end, BMDMs were polarized toward a pro-resolution or a pro-inflammatory phenotype, or left unstimulated, and cultured in media at a normal pH of 7.4 or at acidic pH of 6.8 or 6.5; PER2-Luc rhythms were then observed by LumiCycle. In unstimulated and pro-resolution BMDMs, lower pH led to enhanced amplitude, a shortening in period, and increased damping rate of rhythms at pH 6.8 and pH 6.5 relative to neutral pH 7.4 (Figure 2A,B; Supplementary Figure 4A). This suggests that in unstimulated and pro-resolution macrophages, acidic pH can strengthen rhythms by enhancing amplitude and speeding up the circadian clock, but may impair ability to maintain synchrony. Notably, changes in amplitude and period occurred in a dose-dependent fashion as pH decreased, indicating that rhythms are altered in a pH-dependent manner. In contrast, pro-inflammatory macrophages cultured at pH 6.5 exhibited suppressed amplitude, elongated period, and decreased damping rate of rhythms compared to those cultured at pH 7.4 (Figure 2C; Supplementary Figure 4A). This suggests that in pro-inflammatory macrophages, acidic pH can weaken rhythms by decreasing amplitude and slowing down the speed of the clock, but may promote the ability to maintain synchrony. Low pH was also observed to alter the expression of the circadian clock genes *Per2*, *Cry1*, and *Nr1d1* (REV-ERBα) over time across different macrophage phenotypes, confirming that multiple components of the circadian clock are altered by acidic pH (Figure 2D-F). Notably, the patterns in expression of circadian genes did not always

match the patterns of PER2-Luc levels observed by LumiCycle. This is perhaps unsurprising, as circadian rhythms are regulated at multiple levels (transcriptional, post-transcriptional, translational, post-translational); as a result, circadian patterns observed in circadian proteins such as PER2-Luc do not always match those of their gene transcripts[77]. Together, these data indicate that exposure to acidic pH can induce changes in circadian rhythms of macrophages. Interestingly, our data indicate that while rhythms of unstimulated and pro-resolution macrophages are enhanced under acidic pH despite increased damping rate, rhythms of pro-inflammatory macrophages are suppressed under acidic conditions but have improved damping rate. This suggests that acidic pH modulates rhythms differently in macrophage of different phenotypes.

The observation that acidic pH can enhance rhythms is particularly interesting, given that acidic pH is a stressful condition that can compromise macrophage survival (Supplementary Figure 4B)[30]. In line with their documented enhanced glycolytic capacity, pro-inflammatory macrophages acidified the media over time (Supplementary Figure 4C). Notably, while pH of the media the pro-inflammatory macrophages were cultured in decreased over time pH, the pH differential between the pH 7.4, pH 6.8, and pH 6.5 samples groups of pro-inflammatory macrophages was maintained out to 2 days, consistent with the changes in rhythms that we observe and measure between these groups.

While BMDMs are a widely used model for studying macrophages *in vitro*, there are biological differences between BMDMs generated in culture and tissue-resident macrophages. Thus, we sought to determine whether our observations of pH-induced changes in rhythms were relevant to tissue-resident macrophages differentiated *in vivo*. To this end, we harvested peritoneal macrophages from mice expressing PER2-Luc in the morning at ZT0 (6 AM) or in the evening at ZT12 (6 PM). Peritoneal macrophages were cultured in media at neutral pH of 7.4 or acidic pH of 6.5 and observed by LumiCycle.

Recapitulating our results in BMDMs, peritoneal macrophages exhibited increased amplitude, decreased period, and increase rate of damping at pH 6.5 compared to pH 7.4 (Figure 3A). To test whether pH-driven changes in circadian rhythms of peritoneal macrophages were reflected at the mRNA level, we compared expression of circadian clock genes in peritoneal macrophages cultured at neutral pH 7.4 or acidic pH 6.8 for 24 hours using publicly available RNA-sequencing data [30]. In line with altered circadian rhythms observed by Lumicycle, peritoneal macrophages cultured at pH 6.8 expressed different levels of circadian clock genes than peritoneal macrophages culture at pH 7.4 (Figure 3B). The trends in changes of gene expression in peritoneal macrophages cultured at pH 6.8 matched what we observed in BMDMs, where low pH generally led to higher levels of circadian clock gene expression (Figure 2D-F). These data support our observations by LumiCycle and indicate that acidic pH drives transcriptional changes in multiple components of the circadian clock. In all, these data are evidence that pH-dependent changes in circadian rhythms are relevant to *in vivo*-differentiated macrophages.

Circadian rhythms confer time-of-day variability in response to stimuli. As we have observed that acidic pH can influence circadian rhythms of peritoneal macrophages, we sought to understand if peritoneal macrophages would be more or less susceptible to pH-induced changes in rhythms depending on time of day of exposure. To this end, we compared the magnitude of change in amplitude, period, and damping in peritoneal macrophages when exposed to acidic pH 6.5 compared to neutral pH 7.4 at different times of day (Figure 3C). We observed no significant difference in the pH-driven change in amplitude, period, or damping in rhythms of peritoneal macrophages taken in the morning at ZT0 compared to those taken in the evening at ZT12. This indicates that the influence of pH on rhythms of macrophages was similar when exposed to acidic pH in the morning or in the evening, which suggests that macrophages are similarly susceptible to pH-induced changes in rhythms regardless of time of day of exposure.

Lactate alters circadian rhythms of macrophages in a manner distinct from acidic pH.

Elevated lactate concentrations often co-localize to regions of high acidity, due to the export of both protons and lactate by glycolytic cells[89-91]. In tumors, concentration of lactate has been observed to be present in concentrations of up to 30mM, which are elevated over typical lactate levels in blood and healthy tissue of 1.5-3mM[92]. There are previous reports that lactic acid can promote polarization of macrophages toward a pro-resolution phenotype[93]. Thus, we sought to understand if lactate may be a feature of the TME capable of influencing circadian rhythms of macrophages, in addition to acidic pH. To this end, we cultured BMDMs in the presence or absence of 25 mM sodium-L-lactate. In line with previous observations, BMDMs exposed to lactate had elevated levels of *Vegf*; however, we did not observe significant elevation of *Arg1* (Figure 4A)[93].

We next cultured BMDMs at normal pH 7.4 or acidic pH 6.5, in the presence or absence of 25 mM sodium-L-lactate, and monitored circadian rhythms (Figure 4B,C). Rhythms of BMDMs at pH 7.4 exposed to lactate had an elongated period and decreased damping time compared to BMDMs cultured at pH 7.4 without lactate (Figure 4B). This suggests that lactate can slow the circadian clock and may impair the ability of macrophages to maintain synchrony. Interestingly, these changes in rhythms are different from those observed in acidic conditions, indicating that lactate can modulate circadian rhythms in macrophages in a manner distinct from acidic pH.

As previously observed, macrophages exposed to acidic pH 6.5 exhibited increased amplitude, shortened period, and increased damping rate of circadian rhythms. When BMDMs were exposed to both acidic pH and elevated lactate, the increased amplitude observed at pH 6.5 is maintained; however, the shortened period observed at pH 6.5 is lost, with period lengthened in BMDMs cultured in 25 mM sodium-l-lactate.

296 The increased damping rate of rhythms in BMDMs cultured at pH 6.5 compared to pH 7.4 is maintained,
297 and is further dampened by exposure to lactate. These data indicate that changes in rhythms associated
298 with acidic conditions persisted when co-exposed to elevated lactate. Lactate was also observed to alter
299 expression of the circadian clock genes *Per2*, *Cry1*, and *Nr1d1* over time in BMDMs cultured at pH 6.5,
300 while having more subtle effects at pH 7.4 (Figure 4C). Notably, lactate blunted the effect of pH 6.5 on
301 *Cry1* expression, while enhancing the effect of low pH on *Nr1d1* expression. In all, these data indicate
302 that concentration of lactate similar to that present in the TME can influence circadian rhythms and
303 circadian clock gene expression of macrophages. Lactate altered rhythms differently than acidic pH, and
304 when macrophages were exposed to acidic pH and lactate together, rhythms were further altered. This
305 suggests that when macrophages are exposed to multiple conditions capable of altering circadian
306 rhythms, each condition may contribute to a combined effect on rhythms that differs from its individual
307 impact.
308
309 **Cancer cell supernatant alters circadian rhythms in macrophages in a manner partially reversed by**
310 **neutralization of pH.**
311
312 We have observed that polarizing stimuli, acidic pH, and lactate can alter circadian rhythms. However,
313 the tumor microenvironment is complex. Cancer cells secrete a variety of factors and deplete nutrients
314 in the environment. To model this, we cultured BMDMs in RPMI or supernatant collected from KCKO
315 cells, which are a murine model of pancreatic ductal adenocarcinoma (PDAC)[94, 95], at pH 6.5 or
316 neutralized to pH 7.4 (Supplementary Figure 5). Circadian rhythms of BMDMs cultured in cancer cell
317 supernatant at pH 7.4 or pH 6.5 exhibited increased amplitude and lengthened period compared to
318 RPMI control at pH 7.4 or 6.5, respectively, indicating that cancer cell supernatant contains factors that
319 can alter circadian rhythms of BMDMs. Notably, BMDMs cultured in cancer cell supernatant at pH 6.5

had increased amplitude and shortened period compared to BMDMs cultured in cancer cell-conditioned media at pH7.4, indicating that pH-driven changes in rhythms were maintained in BMDMs cultured in cancer cell supernatant. When the pH of cancer cell supernatant was neutralized to pH7.4, the increased amplitude was decreased, and the shortened period was lengthened, indicating that neutralizing acidic pH partially reverses the changes in rhythms observed in macrophages cultured in cancer cell supernatant at pH 6.5. These data further support our observations that acidic pH can alter circadian rhythms of macrophages both alone and in combination with various factors in the TME.

Induction of cAMP signaling alone is not sufficient to fully drive changes in circadian rhythms associated with acidic pH.

Evidence in the literature suggests that acidic pH is primarily sensed by macrophages via certain G protein-coupled receptors (GPCRs), inducing an increase in intracellular cAMP that drives downstream signaling through the cAMP pathway[29]. Transcriptional changes downstream of cAMP signaling subsequently promote a pro-resolution phenotype[29, 96, 97]. Transcription of the *Crem* isoform *Icer* is also induced downstream of cAMP signaling, and has been used as a "biomarker" for macrophages exposed to acidic conditions in tumors[29]. In line with previous reports, we have observed induction of *Icer* in macrophages under acidic pH (Supplementary Figure 3B), suggesting that cAMP signaling is being induced under acidic conditions [29]. This occurs as early as 2 hours, concurrent with changes in rhythms, which are observed by 6 hours following exposure to acidic conditions. It has been shown that induction of cAMP signaling alone is sufficient to drive a pro-resolution phenotype in macrophages similar to that observed under acidic conditions[29, 96]. Additionally, cAMP signaling has been previously observed to modulate circadian rhythms in SCN and rat fibroblasts[98, 99]. Thus, we sought to

understand if the cAMP signaling pathway may be mediating the pH-induced changes in circadian rhythms in macrophages.

The synchronization protocol we use to study circadian rhythms in BMDMs involves a 24-hour period of serum starvation followed by 2 hours of serum shock. It has previously been shown that serum shock can induce signaling through the cAMP pathway in rat fibroblasts[98]. To determine whether the synchronization protocol impacts cAMP signaling in macrophages, we harvested macrophages before and after serum shock. We then assessed *Icer* expression and phosphorylation of cyclic AMP-response element binding protein (CREB), which occur downstream of cAMP and have been used as readouts to assess induction of cAMP signaling in macrophages[29, 96, 100]. Serum shock of macrophages following serum starvation led to rapid phosphorylation of CREB and *Icer* expression that quickly returned to baseline (Supplementary Figure 2D,E). This indicates that serum starvation followed by serum shock in the synchronization protocol we use to study circadian rhythms in BMDMs induces transient signaling through the cAMP signaling pathway.

As acidic pH induces signaling through the cAMP pathway, we sought to determine whether acidic pH independently contributed to the pH-driven changes in circadian rhythms we observe in BMDMs. To test this, we omitted the synchronization step and observed BMDM rhythms by LumiCycle when cultured in neutral pH 7.4 or acidic pH 6.8 or pH 6.5 (Supplementary Figure 6). Circadian rhythms of BMDMs cultured at pH 6.5 exhibited similar changes as previously observed, with enhanced amplitude and shortened period relative to BMDMs at pH 7.4. This indicates pH-driven changes observed in circadian rhythms of BMDMs occur in the absence of prior serum starvation and serum shock.

To determine if elevation in intracellular cAMP alone was sufficient to drive changes in rhythms observed in macrophages under acidic conditions, we treated macrophages with forskolin, an adenylyl cyclase activator that stimulates production of cAMP, or 3-isobutyl-1-methylxanthine (IBMX), which drives accumulation of cAMP through inhibition of phosphodiesterases (PDEs). We used a range of doses similar to those previously shown to induce cAMP signaling in macrophages in the literature[29, 98, 100]. Treatment with either forskolin or IBMX increased amplitude of rhythms in macrophages, but not to the same magnitude as acidic pH, and did not result in a changed period (Figure 5A,B). Moreover, amplitude of rhythms was not altered in forskolin- or IBMX-treated macrophages at pH 6.5, indicating that neither forskolin nor IBMX had any additional effect on rhythms under acidic conditions. These data indicate that in macrophages, cAMP signaling alone induces enhanced amplitude of rhythms similar to low pH, but the magnitude of this change is far less; additionally, period, which is altered under acidic conditions, remains unchanged. This suggests that cAMP signaling may contribute to but is not sufficient to fully recapitulate the changes in rhythms observed under acidic conditions.

Adenylyl cyclase inhibitor MDL-12330A suppresses pH-mediated changes in amplitude of circadian rhythms and pro-resolution phenotype without suppressing cAMP signaling.

To further test whether pH-induced changes in rhythms are mediated by cAMP signaling, we treated BMDMs with MDL-12330A (henceforth referred to as MDL-12), an adenylyl cyclase inhibitor which has previously been shown to suppress cAMP signaling in macrophages under acidic conditions[29]. When BMDMs cultured at pH 6.5 were treated with MDL-12, the elevated amplitude of rhythms observed at pH 6.5 was suppressed (Figure 5C). Notably, this occurred in a dose-dependent manner, suggesting that this is a drug-dependent effect. Importantly, rhythms of MDL-12-treated macrophages at pH 7.4 had similar amplitude to vehicle-treated macrophages at pH 7.4. This suggests that the inhibitory effect of

MDL-12 on pH-induced enhancement of amplitude in macrophage rhythms was specific to acidic conditions. However, MDL-12 treatment of macrophages at pH 7.4 resulted in shortened period and decreased damping rate compared to vehicle-treated macrophages. Together, MDL-12-mediated suppression of pH-driven changes in amplitude, but not period or damping, suggests that the pH-driven changes in these different parameters of rhythms may occur through different pathways. Interestingly, although the adenylyl cyclase inhibition by MDL-12 is reported to be irreversible, we found that pretreatment up to 2 hours was not sufficient to suppress pH-induced changes in amplitude (Supplementary Figure 7). Only when macrophages continued to be cultured with MDL-12 while exposed to acidic conditions was amplitude suppressed. Meanwhile, co-treating cells with acidic pH and MDL12 without any pre-treatment was sufficient to suppress elevation of amplitude under acidic conditions (Figure 5C).

Evidence suggests that acidic pH signals through the cAMP pathway to promote a pro-resolution phenotype in macrophages, with induction of *Icer* occurring directly downstream of cAMP signaling[29]. Despite preventing changes in amplitude under acidic pH, MDL12 treatment at the dose and treatment schedule used does not suppress induction of *Icer* in macrophages under acidic conditions (Figure 5D). However, induction of *Arg1* expression in macrophages under acidic conditions was suppressed by MDL-12. This suggests that at the dose and treatment strategy used, MDL-12 partially suppresses the response of macrophages to acidic pH by suppressing the pH-driven polarization toward a pro-resolution phenotype and changes in amplitude.

To further investigate how MDL-12 was influencing cAMP signaling at the dose and treatment strategy used, we evaluated phosphorylation of cyclic AMP-response element binding protein (CREB). Phosphorylation of CREB occurs downstream of cAMP and has commonly been used as a readout to

assess induction of cAMP production in macrophages[96, 100]. In line with evidence in the literature that exposure to acidic pH drives an increase in intracellular cAMP in macrophages[29], we observed that downstream phosphorylation of CREB was elevated in macrophages exposed to acidic pH compared to those in non-acidic conditions (Figure 5E,F). Unexpectedly, pCREB levels remained elevated in BMDMs at pH 6.5 despite treatment with MDL-12, indicating that pH-driven phosphorylation of CREB was not suppressed by MDL12 treatment. In fact, pCREB was elevated in MDL-12-treated BMDMS at pH 7.4, suggesting that MDL-12 treatment alone induced phosphorylation of CREB. This is particularly surprising considering that amplitude was not altered in MDL-12-treated macrophages at neutral pH 7.4 despite elevated pCREB. This suggests that some elements of the cAMP signaling pathway, such as pCREB, may be divorced from the pH-induced changes in rhythms. Collectively, our data indicate that while the cAMP signaling pathway is induced under acidic conditions, pH-induced changes in rhythms may not be attributed to cAMP signaling alone, as MDL-12 treatment suppressed pH-induced changes in amplitude of rhythms, but not period or damping, without suppressing signaling through the cAMP pathway.

There is evidence of circadian disorder in the tumor-associated macrophage population.

As we have observed that acidic pH at levels commonly observed in the TME can alter circadian rhythms in macrophages *in vitro* and *ex vivo*, we next sought to investigate whether circadian rhythms can be altered in the TME *in vivo*. Using publicly available data, we analyzed gene expression of tumor-associated macrophages (TAMs) isolated from LLC (Lewis Lung carcinoma) tumors in mice [101]. As a positive control for circadian clock disruption, we used data from BMAL1 KO peritoneal macrophages [44]. BMAL1 KO macrophages have a genetic disruption of the circadian clock due to the loss of Bmal1, the central clock gene. As a result, circadian rhythms of BMAL1 KO macrophages are disrupted, lacking rhythmicity and downstream circadian regulation of macrophage function (Supplementary Figure 8)[45,

54]. In line with previous observations, TAMs had elevated expression of *Arg1* relative to WT and BMAL1 KO peritoneal macrophages (Figure 6A). Expression of *Crem*, which encodes *Icer*, was also elevated in TAMs, indicating that these TAMs were exposed to acidic conditions within the TME (Figure 6A)[29].

To understand the status of the circadian clock in TAMs, we performed clock correlation distance (CCD) analysis. This analysis has previously been used to assess functionality of the circadian clock in whole tumor and in normal tissue[102]. As the circadian clock is comprised of a series of transcription/translation feedback loops, gene expression is highly organized in a functional, intact clock, with core clock genes existing in levels relative to each other irrespective of the time of day. In a synchronized population of cells, this ordered relationship is maintained at the population level, which can be visualized in a heatmap. CCD is designed to compare circadian clock gene co-expression patterns between different tissues and cell types. To accomplish this, CCD was built using datasets from multiple different healthy tissues from mouse and human to be a universal tool to compare circadian rhythms. Each sample is compared to a reference control built from these multiple tissues (Figure 6B)[102]. To validate the use of this analysis for assessing circadian disorder in macrophages, we performed CCD analysis using publicly available RNA-sequencing data from bone marrow-derived macrophages and wild type peritoneal macrophages, as a healthy control for functional rhythms in a synchronized cell population, and BMAL1 KO peritoneal macrophages, as a positive control for circadian disorder[44]. We found that gene co-expression of clock genes was ordered in wild type macrophages with functional clocks and intact circadian rhythms (Figure 6C, Supplementary Figure 8). In contrast, clock gene co-expression is disordered in BMAL1 KO macrophages with a genetic disruption of the circadian clock, leading to disruption of circadian rhythms (Figure 6C,D, Supplementary Figure 8). This indicates that CCD analysis can be used to measure circadian disorder in a macrophage population. To assess the status of the circadian clock in tumor-associated macrophages, we next performed CCD analysis using RNA-

462 sequencing data of TAMs derived from LLC tumors[101]. Clock correlation distance analysis revealed
463 that, similar to the BMAL1 KO peritoneal macrophages, the co-expression relationship between the core
464 circadian clock genes in TAMs is significantly more disordered than that of WT peritoneal macrophages
465 (Figure 6C,D). Weighted gene co-expression network analysis (WGCNA) has been used as an alternate
466 approach to measure the co-variance between clock genes and thus assess bi-directional correlations
467 among the core clock gene network in healthy tissue and tumor samples [103]. In line with the circadian
468 disorder observed by CCD, while many bi-directional correlations among the core clock gene network
469 were significant and apparent in wild type peritoneal macrophages, these relationships were altered or
470 abolished within BMAL1 KO peritoneal macrophages and TAM samples, and in some cases replaced by
471 new relationships (Figure 6E). This indicates that there is population-level disorder in the circadian
472 rhythms of tumor-associated macrophages in murine lung cancer.
473
474 We next assessed the status of the circadian clock in human TAMs from NSCLC patients. We performed
475 CCD with publicly available RNA-seq data of tumor-adjacent macrophages and tumor-associated
476 macrophages from NSCLC patients, using alveolar macrophages from healthy donors as a control[104,
477 105]. To assess the contribution of the acidic TME to circadian disorder, we subset TAM NSCLC patient
478 samples into groups (*Crem* high TAMs and *Crem* low TAMs) based on median *Crem* expression. Notably,
479 in macrophages from human NSCLC there was a trend toward disorder in *Crem* low but not *Crem* high
480 TAM samples (Figure 7A,B). Additionally, the co-variance among core clock genes observed in alveolar
481 macrophages from healthy donors was absent within *Crem* low and *Crem* high TAM samples (Figure 7C).
482 In all, these data indicate that there is population-level disorder in the circadian rhythms of tumor-
483 associated macrophages in humans and mice, suggesting that circadian rhythms are indeed altered in
484 macrophages within the TME.
485

Heterogeneity of circadian rhythms within a population can underlie circadian disorder as measured by CCD.

Circadian disorder assessed by CCD has previously been used to infer disruption of circadian rhythms[106]. Indeed, we observed that genetic disruption of circadian rhythms by BMAL1 KO resulted in a disordered clock, as observed in peritoneal macrophages (Figure 6B). However, since CCD is a population-level analysis, heterogeneity of rhythms, as observed in a desynchronous cell population, rather than disruption of rhythms, may also underlie the circadian disorder observed by CCD. Heterogeneity in macrophage phenotype, exposure to acidic pH, and lactate are all factors present in the TME and relevant to tumor-associated macrophages. We have observed that each of these factors can alter circadian rhythms in macrophages, both alone and in combination with each other. Furthermore, we have observed a trend toward circadian disorder in *Crem* low TAM samples but not *Crem* high TAM samples. Thus, we sought to understand if heterogeneity in macrophage rhythms could be contributing to the disorder in clock gene co-expression and poor CCD score indicative of population-level disorder in TAM rhythms.

To address this, we examined if differences in rhythms of macrophages within a population might contribute to population-level disorder as measured by CCD. To this end, we used publicly available data of peritoneal macrophages taken at different times of day in four-hour intervals across two days[36]. We then constructed four different sample groups in which samples were pooled according to time of day of harvest. As a control for a synchronized cell population with homogenous rhythms, samples taken at the same time of day were pooled. We then modeled a progressively desynchronized population with increased differences in phase of rhythms by pooling samples that were taken four hours apart, eight hours apart, or twelve hours apart (Figure 8A). CCD was then performed on these four populations

(Figure 8B). CCD score worsened as populations became increasingly desynchronized, with the 12hr desynchronized population having a significantly worse CCD score than synchronized, homogenous macrophage population (Figure 8C). This indicates that as circadian rhythms of individual macrophages within a population become more different from each other, circadian disorder increases at the population-level. This is further supported by WGCNA, which revealed that the significant co-variance of circadian clock genes in the synchronized population was progressively altered and lost as the population is increasing desynchronized to 12 hours (Supplementary Figure 9). The results of these analyses suggests that heterogeneity in rhythms, as observed with desynchrony, may underlie population-level disorder of the circadian clock as measured by CCD.

Tumor-associated macrophages exhibit heterogeneity in circadian clock gene expression.

Our findings suggested that heterogeneity of the circadian clock may lead to disorder in bulk macrophage populations, but did not reveal if specific gene expression changes exist in tumor-associated macrophages at the single-cell level. To determine whether heterogeneity exists within the expression of circadian clock genes of the tumor-associated macrophage population, we analyzed publicly available single-cell RNA sequencing data of macrophages isolated from B16-F10 tumors[107]. To capture the heterogeneity of macrophage subsets within the TAM population, we performed unbiased clustering (Figure 9A). We then performed differential gene expression to determine if circadian clock genes were differentially expressed within the TAM subpopulations. The circadian clock genes *Bhlhe40* (DEC1), *Bhlhe41* (DEC2), *Nfil3* (E4BP4), *Rora* (RORα), *Dbp* (DBP), and *Nr1d2* (REV-ERBβ) were significantly (adj.p<0.005) differentially expressed between TAM clusters (Figure 9B). This indicates that there is heterogeneity in expression of circadian clock genes within the TAM population.

We next sought to determine whether differences in circadian clock gene expression between TAM subpopulations were associated with exposure to acidic pH in the TME. To this end, we first assessed *Crem* expression in the TAM subpopulations that were identified by unbiased clustering. *Crem* expression was significantly higher in TAM clusters 4, 5, and 6 compared to TAM clusters 1-3 and 7-9 (Figure 9C). Clusters were subset based on *Crem* expression into *Crem* high (clusters 4-6) and *Crem* low (clusters 1-3, 7-9) (Figure 9D), and differential gene expression analysis was performed. The circadian clock genes *Nfil3, Rora, Bhlhe40,* and *Cry1* (CRY1) were significantly (adj.p<0.005) differentially expressed between *Crem* high and *Crem* low TAMs (Figure 9E). This suggests that acidity within the TME is associated with heterogeneity in expression of circadian clock genes within the TAM population. Interestingly, expression of circadian clock genes varied between clusters designated as *Crem* high or *Crem* low (Figure 9B); for instance, *Nfil3* was more highly expressed in cluster 1 than cluster 3, both of which had low *Crem* expression. This indicates that there is diversity in circadian clock gene expression within the *Crem* high and *Crem* low groups, suggesting that acidic pH is not the only factor in the TME that can alter the circadian clock. Collectively, these data suggest that there is heterogeneity in the circadian clock of macrophages within the TAM population that is driven in part by acidic pH.

Circadian rhythms of macrophages can influence tumor growth in a murine model of pancreatic cancer.

We next sought to determine how circadian rhythms in tumor-associated macrophages may influence tumor growth in KCKO, a murine model of PDAC [94, 95]. To this end, we used a genetic disruption of the circadian clock in macrophages. Myeloid-specific genetic mouse models are not macrophage-specific, so co-injection experiments are commonly used to determine macrophage-specific roles[93, 108-110]. Thus, we co-injected BMDMs from WT or BMAL1 KO mice along with KCKO cells into WT mice, and

558 tumor growth was measured. We saw a significant increase in the growth of tumors co-injected with
559 BMAL1 KO macrophages compared to those co-injected with WT macrophages (Figure 10). These results
560 suggest intact circadian rhythms of macrophages can restrain tumor growth, in agreement with similar
561 published findings in a murine model of melanoma[109].
562

563 Discussion

564

565 Macrophages experience altered environmental conditions within the tumor microenvironment, but
566 how these may affect macrophage circadian rhythms remains unclear. Here we assessed whether
567 circadian rhythms are altered in macrophages within the TME. To this end, we investigated whether
568 conditions commonly associated with the tumor microenvironment could influence circadian rhythms in
569 macrophages. As TAMs are phenotypically heterogenous, we first assessed circadian rhythms in
570 macrophages polarized toward different phenotypes. We found that polarization state affected circadian
571 rhythmicity, with pro-inflammatory macrophages exhibiting far weaker rhythms that pro-resolution
572 macrophages (Figure 1). We then modeled acidic conditions in the TME by exposing macrophages to pH
573 and lactate levels similar to those found in the TME, and found that low pH in particular dramatically
574 altered the rhythms of macrophages (Figures 2-4). Changes in cAMP signaling may contribute to these
575 changes in rhythmicity, but low pH induced alterations far beyond what is observed by enhancing cAMP
576 signaling pharmacologically (Figure 5A,B). While the adenylyl-cyclase inhibitor MDL-12 largely rescued
577 the changes in amplitude observed in low pH, our data suggest that a pathway other than canonical
578 cAMP signaling may be involved in this effect (Figure 5C-F). Finally, we assessed the status of the
579 circadian clock in tumor-associated macrophages, the potential contribution of heterogeneity in
580 circadian rhythms to population-level rhythms, and assessed whether the circadian regulation of
581 macrophages impacts tumor growth. Our results indicated that macrophage rhythms are disordered

582 within tumors (Figure 6,7), and that heterogeneity in rhythms within the tumor-associated macrophage
583 population may underlie this observed circadian disorder (Figure 8), which was supported by our
584 observations of heterogeneity in circadian clock gene expression within the TAM population from scRNA-
585 seq data (Figure 9). We further demonstrated that the intact macrophage circadian clock can suppress
586 tumor growth (Figure 10). Overall, our results for the first time demonstrate that exposure of
587 macrophages to conditions associated with the tumor microenvironment can influence circadian
588 rhythms, a key aspect of macrophage biology.
589
590 A critical question in understanding the role of circadian rhythms in macrophage biology is determining
591 how different polarization states of macrophages affect their internal circadian rhythms. This is especially
592 important considering that tumor-associated macrophages are a highly heterogeneous population. Our
593 data indicate that compared to unstimulated macrophages, rhythms are enhanced in pro-resolution
594 macrophages, characterized by increased amplitude and improved ability to maintain synchrony; in
595 contrast, rhythms are suppressed in pro-inflammatory macrophages, characterized by decreased
596 amplitude and impaired ability to maintain synchrony (Figure 1). These agree with previously published
597 work showing that polarizing stimuli alone and in combination with each other can alter rhythms
598 differently in macrophages[80, 81]. In a tumor, macrophages exist along a continuum of polarization
599 states and phenotypes[18-21, 24]. Thus, while our characterizations of rhythms in *in vitro*-polarized
600 macrophages provide a foundation for understanding how phenotype affects circadian rhythms of
601 macrophages, further experiments will be needed to assess macrophages across the full spectrum of
602 phenotypes. Indeed, alteration of rhythms may be just as highly variable and context-dependent as
603 phenotype itself.
604

In addition to polarizing stimuli, tumor-associated macrophages are exposed to a variety of conditions within the tumor microenvironment that may alter their circadian rhythms. We observed that exposure to acidic pH altered rhythms in macrophages, increasing amplitude of pro-resolution macrophages but suppressing amplitude of pro-inflammatory macrophages (Figure 2). This indicates that pH affects rhythms differently depending on phenotype, hinting at additional layers of complexity in how the environment could contribute to changes in circadian rhythms. Even further changes in rhythms were observed when macrophages were exposed to lactate in conjunction with acidic pH (Figure 4). These observations suggest that the combination of stimuli present in the microenvironment such as lactate and low pH, as well as various polarizing stimuli, can each contribute to modulate rhythms, resulting in highly context-dependent changes in circadian rhythms of macrophages based on the microenvironment. As macrophages are highly plastic and exquisitely capable of sensing and responding to their environment, one could reason that changes in circadian rhythms, and downstream circadian regulation, are a mechanism by which macrophages can adopt different programs to respond to their environment.

Elucidating the role of circadian rhythms in regulation of macrophage biology necessitates a better understanding of the crosstalk between phenotype and circadian rhythms. Although lactate polarizes macrophages toward a pro-resolution phenotype similar to acidic pH[30, 93], exposure to lactate had different effects on circadian rhythms – and in some cases, circadian clock gene expression – than exposure to acidic pH (Figure 4). Sensing of lactate occurs through different pathways than acid-sensing, which may contribute to the different ways in which these two stimuli modulate circadian rhythms of macrophages[111]. One previously published finding that may offer mechanistic insight into how phenotype can influence circadian rhythms is the suppression of Bmal1 by LPS-inducible miR-155[54]. It has also been observed that RORα-mediated activation of Bmal1 transcription is enhanced by PPARγ co-

activation[112]. In macrophages, PPARγ expression is induced upon stimulation with IL-4 and plays a key role in alternative activation of macrophages, promoting a pro-resolution macrophage phenotype, and supporting resolution of inflammation[113-115]. Such observations prompt the question of whether there are yet-unidentified factors induced downstream of various polarizing stimuli that can modulate expression of circadian genes at the transcriptional and protein levels. Further work is required to understand the interplay between macrophage phenotype and circadian rhythms.

It was previously observed that acidic pH can disrupt circadian rhythms in cell lines[32]. However, while acidic pH altered rhythms in macrophages, it did not ablate them. This suggests that the influence of acidic pH on circadian rhythms can vary between cell types. pH-induced circadian disruption was found to be driven by inhibition of mTORC1 activity in cell lines, and there was evidence to suggest that mTORC1 activity was sensitive to pH in T cells [116]. Thus, the role of mTORC1 activity in mediating pH-driven changes in circadian rhythms of macrophages will be a topic of future investigation.

The mechanism through which acidic pH can modulate the circadian clock in macrophages remains unclear. Evidence in the literature suggests that acidic pH promotes a pro-resolution phenotype in macrophages by driving signaling through the cAMP pathway[29]. It has previously been shown that cAMP signaling can modulate the circadian clock[99]. However, our data indicated that cAMP signaling was not fully sufficient to confer pH-mediated changes in circadian rhythms of macrophages (Figure 5A,B). Treatment with MDL-12, commonly known as an inhibitor of adenylyl cyclase[29, 117], resulted in suppression of pH-induced changes in amplitude of circadian rhythms but did not inhibit signaling through the cAMP signaling pathway (Figure 5C,D). While MDL-12 is commonly used as an adenylyl cyclase inhibitor, it has also been documented to have inhibitory activity toward phosphodiesterases (PDEs) and the import of calcium into the cytosol through various mechanisms[118, 119]. This is of

653 particular interest, as calcium signaling has also been shown to be capable of modulating the circadian
654 clock[120]. Furthermore, while acid-sensing through GPCRs have been the most well-characterized
655 pathways in macrophages, there remain additional ways in which acidic pH can be sensed by
656 macrophages such as acid-sensing ion channels[121, 122]. Further work is required to understand the
657 signaling pathways through which pH can influence macrophage phenotype and circadian rhythms.
658
659 We observed that acidic pH appears to enhance circadian rhythms of unstimulated and pro-resolution
660 macrophages, and we and others have shown evidence that macrophages are exposed to an acidic
661 environment within the TME[28, 29]. Interestingly, analysis of TAMs by clock correlation distance (CCD)
662 presents evidence that rhythms are disordered in bulk TAMs compared to other macrophage
663 populations (Figure 6). CCD is one of the most practical tools currently available to assess circadian
664 rhythms due to its ability to assess rhythms independent of time of day and without the need for a
665 circadian time series, which is often not available in publicly available data from mice and humans[102].
666 However, CCD is limited in that it is a measure of population-level circadian rhythms. Our data indicate
667 that heterogeneity of circadian rhythms within a given population can underlie circadian disorder
668 observed by CCD (Figure 8). Indeed, we observed differences in the circadian clock of *Crem* low human
669 TAM samples compared to *Crem* high human TAM samples, suggesting that acidic pH influences
670 circadian disorder in TAMs (Figure 7). Interestingly, *Crem* low TAM samples exhibited a trend toward
671 disorder while *Crem* high TAM samples did not. This is of particular interest, as we have observed that
672 acidic pH can enhance circadian rhythms in macrophages, raising the question of whether acidic pH
673 promotes or protects against circadian disorder. We have shown that various stimuli can alter rhythms of
674 macrophages in a complex and contributing manner, including polarizing stimuli, acidic pH, and lactate.
675 TGFβ is produced by a variety of cells within the TME, and was recently identified as a signal that can
676 modulate circadian rhythms[123, 124]. Additionally, when we exposed macrophages to cancer cell-

conditioned media, rhythms were modulated in a manner distinct from acidic pH or lactate, with these changes in rhythms partially reversed by neutralization of the cancer cell-conditioned media pH (Supplementary Figure 5). It is conceivable that, in addition to acidic pH, other stimuli in the TME are influencing circadian rhythms to drive population-level disorder that we observed by CCD.

Supporting the notion that population-level disorder may exist in TAMs, we used scRNA-sequencing data and found evidence of heterogeneity between the expression of circadian clock genes in different TAM subpopulations (Figure 9A, B). Phenotypic heterogeneity of TAMs in various types of cancer has previously been shown[20, 21, 125, 126], and we have identified distinct TAM subpopulations by unbiased clustering (Figure 9A). Within those TAM subpopulations, we identified differential expression of circadian clock genes encoding transcription factors that bind to different consensus sequences: DEC1 and DEC2 bind to E-boxes, NFIL3 and DBP binds to D-boxes, and RORα and REV-ERBβ binds to retinoic acid-related orphan receptor elements (ROREs)[127, 128]. While little is known about regulation of macrophages by E-box and D-box elements beyond the circadian clock, aspects of macrophage function have been shown to be subject to transcriptional regulation through ROREs[129, 130]. Thus, we speculate that variations in these transcription factors may exert influence on expression of genes to drive diversity between TAM subpopulations. Differential expression of circadian clock genes between TAM subpopulations was also associated with *Crem* expression (Figure 9C-E), suggesting that exposure of TAMs to acidic pH within the TME can alter the circadian clock. However, there remained significant variation in expression of circadian clock genes within the *Crem* high and *Crem* low groups (Figure 9B), suggesting that acidic pH is not the only factor in the TME that can alter the circadian clock. Together, these data implicate the TME in driving heterogeneity in TAM circadian rhythms just as it drives heterogeneity in TAM phenotype.

Interestingly, in contrast to our observations of circadian disorder in TAMs isolated from LLC tumors (Figure 6), rhythmicity in expression of circadian genes was observed in bulk TAMs isolated from B16 tumors[107]. This suggests that circadian rhythms of TAMs are maintained differently in different types of cancer. Notably, both of these observations were at the population level. Upon separation of the B16 TAM population into subsets by unbiased clustering of single-cell RNA sequencing data, we measured differences in expression of circadian clock genes between TAM subpopulations (Figure 9A,B). This suggests that even within a rhythmic TAM population, there is heterogeneity in the circadian clock of TAM subpopulations.

Considering our observations that conditions associated with the TME can alter circadian rhythms in macrophages, it becomes increasingly important to understand the relevance of macrophage rhythms to their function in tumors. It has been shown that acidic pH and lactate can each drive functional polarization of macrophages toward a phenotype that promotes tumor growth, with acidic pH modulating phagocytosis and suppressing inflammatory cytokine secretion and cytotoxicity[28, 30, 93]. However, how the changes in circadian rhythms of macrophages driven by these conditions contributes to their altered function remains unknown. Current evidence suggests that circadian rhythms confer a time-of-day-dependency on macrophage function by gating the macrophage response to inflammatory stimuli based on time-of-day. As such, responses to inflammatory stimuli such as LPS or bacteria are heightened during the active phase while the inflammatory response is suppressed during the inactive phase. An important future direction will be to determine how changes in circadian rhythms of macrophages, such as those observed under acidic pH or high lactate, influences the circadian gating of their function. Data from our lab and others suggest that disruption of the macrophage-intrinsic circadian clock accelerates tumor growth, indicating that circadian regulation of macrophages is tumor-suppressive in models of PDAC (our work) and melanoma [109]. This agrees with complementary

findings that behavioral disruption of circadian rhythms in mice (through chronic jetlag) disrupts tumor macrophage circadian rhythms and accelerates tumor growth[56]**.** It remains unclear whether this is through the pro-tumorigenic functions of macrophages such as extracellular matrix remodeling or angiogenesis, through suppression of the anti-tumor immune response, or a combination of both functions. Further work will be needed to tease apart these distinctions.

Whereas much work has been done to characterize how macrophages are regulated within the TME, the impact of the TME on circadian rhythms of macrophages remained elusive. Our work uncovers a novel way in which conditions associated with the TME can influence macrophage biology through modulation of circadian rhythms. While the majority of studies investigating the circadian regulation of macrophages have been conducted studying macrophages under homeostatic conditions or in response to acute inflammation[36, 38, 44, 45, 131], our work contributes to an emerging body of evidence that the tissue microenvironment can influence circadian rhythms[123]. This is increasingly important when considering the role of circadian rhythms in immune responses at sites of ongoing, chronic inflammation where the microenvironment is altered, such as within tumors. In identifying factors within the TME that can modulate circadian rhythms of macrophages and uncovering evidence of circadian disorder within tumor-associated macrophages, our work lays the foundation for further studies aimed at understanding how the TME can influence the function of tumor-associated macrophages through modulation of circadian rhythms.

Limitations of the Study

Our observations of rhythms in macrophages of different phenotypes are limited by *in vitro* polarization models. It is important to note that while our data suggest that pro-inflammatory macrophages have

suppressed rhythms and increased rate of desynchrony, it remains unclear the extent to which these findings apply to the range of pro-inflammatory macrophages found *in vivo*. We use IFNγ and LPS co-treatment *in vitro* to model a pro-inflammatory macrophage phenotype that is commonly referred to as 'M1', but under inflammatory conditions *in vivo*, macrophages are exposed to a variety of stimuli that result in a spectrum of phenotypes, each highly context-dependent. The same is true for for 'M2'; different tissue microenvironment are different and pro-resolution macrophages exist in a spectrum. Rhythms were heavily suppressed in pro-inflammatory macrophages, which makes analysis of rhythm parameters in pro-inflammatory macrophages more challenging as amplitude and signal reaches limit of detection. Our observations of changes in amplitude and period in pro-inflammatory macrophages compared to unstimulated macrophages agrees with the literature, where these changes in rhythms have been observed using LumiCycle as well as by mRNA[80, 81]. This supports the validity and reproducibility of our observations despite the challenges of observing and analyzing rhythms of pro-inflammatory macrophages.

Methods

Animals

Mice were maintained in individually ventilated cages with bedding and nesting material in a temperature-controlled, pathogen-free environment in the animal care facility at the University of Rochester. All animal protocols were approved by the University of Rochester Committee of Animal Resources (UCAR). All experiments were performed in compliance with the NIH- and University of Rochester-approved guidelines for the use and care of animals, as well as recommendations in the Guide for the Care and Use of Laboratory Animals of the National Research Council[132]. Mice were housed on a 12:12 light dark cycle. In some cases, to ease timepoint collection, mice were housed under reverse lighting conditions in a 12:12 dark light cycle for at least 2 weeks prior to use in experiments. Mice used

for experiments were between the ages of 8-14 weeks old; both male and female mice were used. Mice were euthanized humanely prior to harvesting peritoneal macrophages or bone marrow.

Previously characterized mice with a myeloid-specific deletion of BMAL1 (LysM-cre$^{+/-}$Bmal1$^{flox/flox}$; referred to as BMAL1 KO mice)[45] in a C57BL/6 background were generated by crossing LysM-cre mice[133] with Bmal1$^{flox/flox}$ mice[134]. These mice were further crossed with PER2-Luc mice[76] to generate BMAL1 KO or wild-type control mice (LysM-cre$^{-/-}$Bmal1$^{flox/flox}$; referred to as WT) expressing PER2-Luc. PER2-Luc (strain #006852), LysM-cre (strain #004781), and Bmal1$^{flox/flox}$(strain #007668) mice used for breeding to generate WT and BMAL1 KO mice were purchased from the Jackson Laboratory.

Differentiation and culture of bone marrow-derived macrophages

Bone marrow-derived macrophages (BMDMs) were generated from bone marrow isolated from WT mice using a well-established protocol for differentiation of BMDMs over 7 days[135, 136]. In brief, bone marrow cells were seeded at 200,000 cells/mL on non-tissue culture treated-plates in BMDM Differentiation Media: RPMI (Corning, CAT#MT10040CV) supplemented with 20% (v/v) L929 supernatant and 10% (v/v) heat-inactivated (HI) fetal bovine serum (FBS) (Cytiva, CAT#SH30396.03), supplemented with 100 U/mL Penicillin-Streptomycin (Gibco, CAT# 15140122). Cells were grown at 37^{o}C in air enriched with 5% CO_2. On day 3, additional BMDM Differentiation Media was added to cells. On day 6 of the differentiation protocol, BMDMs were seeded at 1.2*10^{6} cells/mL and left in BMDM Differentiation Media, and kept at 37^{o}C in air enriched with 5% CO_2. On day 7, BMDM Differentiation Media was removed and BMDMs were synchronized.

To synchronize BMDMs, we adapted a recently published method[77]. Briefly, BMDMs were first serum starved for 24 hours in serum-free media (RPMI, supplemented with 100 U/mL Penicillin-Streptomycin);

BMDMs were then subjected to serum shock by replacing serum-free media with RPMI supplemented with 50% (v/V) HI horse serum (Corning, CAT#35030CV) at 37^{o}C in air enriched with 5% CO_2. At the end of this synchronization protocol, media was replaced with Atmospheric Media, which has been formulated for use at atmospheric CO_2 levels and enhanced pH stability by increasing buffering capacity at low pH[32]: RPMI (Corning, CAT#50-020-PC), 25mM HEPES (Gibco, CAT#15630080), 25mM PIPES (Sigma, CAT#P1851), supplemented with 10% (v/v) HI FBS and 100 U/mL Penicillin-Streptomycin[32]. Atmospheric Media was adjusted to pH 7.4, 6.8, or 6.5 with NaOH and filter-sterilized.

BMDMs cultured in Atmospheric Media at pH 7.4, 6.8, or 6.5 were either left unstimulated or were polarized toward a pro-resolution ('M2') or pro-inflammatory phenotype ('M1') by addition of 10 ng/mL IL-4 (PeproTech, CAT#214-14) and 10 ng/mL IL-13 (PeproTech, CAT# 210-13), or 50 ng/mL IFNγ (PeproTech, CAT#315-05) and 100 ng/mL LPS (Invitrogen, CAT#00497693), respectively. For lactate experiments, sodium-L-lactate (Sigma, CAT#L7022) or vehicle was added to Atmospheric Media for 25 mM sodium-L-lactate or 0 mM sodium-L-lactate in Atmospheric Media. For interrogation of cAMP signaling pathway, BMDMs were cultured in Atmospheric Media at pH 7.4 or 6.5 with vehicle or 5, 10, or 15 µM MDL-12330A (Sigma, CAT#M182). For phenocopy experiments (Figure 5), BMDMs were not synchronized prior to the experiment. BMDMs were cultured in Atmospheric Media at pH 7.4 or 6.5 with vehicle or 20, 40, or 80 µM IBMX (Sigma, CAT#I5879) or forskolin (Sigma, CAT#344270). For LumiCycle experiments, 100mM D-luciferin was added to Atmospheric Media at 1:1000 for 100µM D-luciferin (Promega, CAT#E1602). Cells cultured in Atmospheric Media were kept at 37^{o}C in atmospheric conditions, and were either monitored over time by LumiCycle or harvested for RNA or protein at the time points indicated.

Isolation and culture of peritoneal macrophages

Peritoneal exudate cells were harvested from mice as previously published[137]. To isolate peritoneal macrophages, peritoneal exudate cells were seeded at $1.2*10^6$ cells/mL in RPMI/10% HI FBS supplemented with 100U/mL Penicillin-Streptomycin and left at 37°C for 1 hour, after which non-adherent cells were rinsed off[136]. Isolation of peritoneal macrophages using this method has been shown to yield a population that is over 90% in purity[138, 139]. Peritoneal macrophages were then cultured in Atmospheric Media at pH 7.4 or 6.5 with 100µM D-luciferin, and kept at 37°C in atmospheric conditions.

Quantification of circadian rhythm parameters

Using the Lumicycle Analysis program version 2.701 (Actimetrics), raw data was fitted to a linear baseline, and the baseline-subtracted data was fitted to a damped sine wave from which period and damping were calculated[140]. Amplitude was calculated from baseline-subtracted data by subtracting the bioluminescent values of the first peak from the first trough as previously published[80].

Production of KCKO cancer cell supernatant

KCKO cells were seeded at 300,000 cells/mL in pH 7.4 Atmospheric Media (RPMI buffered for use at atmospheric CO_2 levels and enhanced buffering capacity at low pH – see "Differentiation and culture of bone marrow-derived macrophages" section) and cultured at 37°C in atmospheric conditions for 5 days. Supernatant was then collected, pH-adjusted to pH 7.4 or pH 6.5, and filter-sterilized. For the experiment, bone marrow-derived macrophages were cultured in pH 7.4 or pH 6.5 KCKO supernatant, or pH 7.4 or pH 6.5 Atmospheric Media. Media was supplemented with 100 µM D-luciferin, and cells were kept at 37°C in atmospheric conditions and monitored over time by LumiCycle

Quantitative PCR

Cells were lysed and RNA was isolated using the E.Z.N.A. HP Total RNA Kit (Omega BioTek, CAT#R6812-02). RNA was reverse transcribed to cDNA using the ABI Reverse Transcription Reagents system, using oligo dT for priming (Applied Biosystems, CAT#N8080234). qPCR was performed with cDNA using PerfeCTa SYBR Green FastMix (QuantaBio, CAT#95074-05K) and with the Quant Studio 5 quantitative PCR machines (Applied Biosystems). Triplicate technical replicates were performed, outlier replicates (defined as being more than 1 Ct away from other two replicates) were discarded, and relative mRNA was normalized to *Tbp* and assessed by the ΔΔCt. Primers used are in the **Table** below.

Table of primer sequences used

Target	Primer sequences (Forward, Reverse)	Source
Arg1	5'-CTCCAAGCCAAAGTCCTTAGAG-3', 5'-AGGAGCTGTCATTAGGGACATC-3'	[141]
Chil3	5'-AGAAGCAATCCTGAAGACACC-3', 5'-ACTGGTATAGTAGCACATCAGC-3'	IDT Mm.PT.58.33370435
Clec10a	5'-TGACTGAGTTCCTGCCTCT-3', 5'-GACCAAGGAGAGTGCTAGAAG-3'	IDT Mm.PT.56a.19092703
Cry1	5'-GCTATGCTCCTGGAGAGAACG T-3', 5'-TGTCCCCGTGAGCATAGTGTAA-3'	[142]
Icer	5'-ATGGCTGTAACTGGAGATGAA-3', 5'-GTGGCAAAGCAGTAGTAGGA-3'	[29]
Il1b	5'-TACGGACCCCAAAAGATGA-3', 5'-TGCTGCTGCGAGATTTGAAG-3'	[141]
Il6	5'-TAGTCCTTCCTACCCCAATTTCC-3', 5'-TTGGTCCTTAGCCACTCCTTC-3'	[141]

Mrc1	5'-CAAGTTGCCGTCTGAACTGA-3', 5'-TATCTCTGTCATCCCTGTCTCT-3'	IDT Mm.PT.58.42560062
Nos2	5'-GCTTCTGGTCGATGTCATGAG-3', 5'-TCCACCAGGAGATGTTGAAC-3'	IDT Mm.PT.58.43705194
Nr1d1	5'-GAGCCACTAGAGCCAATGTAG-3', 5'-CCAGTTTGAATGACCGCTTTC-3'	IDT Mm.PT.58.17472803
Per2	5'-TGAGGTAGATAGCCCAGGAG-3,' 5'-GCTATGAAGCGCCTAGAATCC-3'	IDT Mm.PT.58.5594166
Retnla	5'-CTGGGTTCTCCACCTCTTCA-3', 5'-TGCTGGGATGACTGCTACTG-3'	[141]
Tbp	5'-CCAGAACTGAAAATCAACGCAG-3', 5'-TGTATCTACCGTGAATCTTGGC-3'	IDT Mm.PT.39a.22214839
Tnfa	5'-ACGGCATGGATCTCAAAGAC-3', 5'-AGATAGCAAATCGGCTGACG-3'	[141]
Vegf	5'-CCACGACAGAAGGAGAGCAGAAGTCC-3', 5'-CGTTACAGCAGCCTGCACAGCG-3'	[93]

Immunoblot

Cells were lysed using the M-Per lysis reagent (Thermo Scientific, CAT#78501), supplemented with protease and phosphatase inhibitor cocktail (1:100; Sigma, CAT#PPC1010) and phosphatase inhibitor cocktail 2 (1:50; Sigma, CAT#P5726), with 200µM deferoxamine (Sigma, CAT#D9533). M-Per is formulated to lyse the nucleus and solubilize nuclear and chromatin-bound proteins, allowing isolation of nuclear proteins as well as cytosolic proteins. Lysates were incubated on ice for 1 hour, then centrifuged at 17,000 xg to pellet out debris; supernatant was collected. Protein was quantified using the

Bio-Rad DC Protein Assay Kit (Bio-Rad, CAT#5000112), and lysates of equal concentration were prepared and run by SDS-PAGE on Bio-Rad Criterion 4–15% Criterion TGX Stain-Free 26-well gradient gel (Bio-Rad, CAT#5678095). Gels were transferred using the Trans-Blot Turbo system (Bio-Rad) to nitrocellulose membranes (Bio-Rad CAT#1704271).

The following primary antibody was used: rabbit anti-p-CREB (Ser133, Ser129) (Invitrogen, CAT#44-297G). The following secondary antibody was used: goat anti-rabbit Alexa Fluor 680 (Invitrogen, CAT#A21109). Of note, two different anti-CREB antibodies were tested (Cell Signaling, CAT#9197 and Invitrogen, CAT#35-0900) in combination with the appropriate secondary antibody, but neither revealed bands at the correct molecular weight for CREB protein. Membranes were digitally imaged using a ChemiDoc MP (Bio-Rad) and uniformly contrasted. Total protein was imaged by Stain-Free imaging technology (Bio-Rad) and used as loading control. To visualize total protein, image of entire membrane was shrunk to match the size of pCREB.

Survival under acidic pH

BMDMs were seeded, in triplicate, at $1.2*10^6$ cells/mL in a 96-well plate. BMDMs were synchronized, then cultured in Atmospheric Media at pH 7.4, 6.8, or 6.5 containing 10 ng/mL IL-4 and 10 ng/mL IL-13, or 50 ng/mL IFNγ and 100 ng/mL LPS, or vehicle for unstimulated control. BMDMs were fixed at 1, 2, and 3 days later. BMDMs were stained with Hoechst (Thermo Scientific, CAT#62259), and plates were imaged using a Celigo S. Number of nuclei per well was enumerated using Celigo software to quantify the number of adherent BMDMs after time in culture under acidic conditions as a readout of survival.

Tumor growth

884 Mice were anesthetized via inhalation of 4 vol% isoflurane (VetOne Fluriso) in 100% oxygen at a flow rate
885 of 4 L/min prior to injection. Following application of 70% ethanol to the site of injection, with $1*10^6$ WT
886 or BMAL1 KO macrophages and $1*10^6$ KCKO cells in 100 uL sterile 0.9% normal saline (Medline,
887 CAT#RDI30296) were subcutaneously co-injected in the flank of WT mice. In line with previously
888 published co-injection tumor experiments, mice were injected with macrophages at a 1:1 ratio[93, 109].
889 Tumor growth was measured by caliper, and volume was calculated by the modified ellipsoidal formula:
890 tumor volume = $0.5*(\text{length}*\text{width}^2)$[143]. Mice were euthanized when there was ulcer formation or
891 when tumor size reached a diameter of 20mm.
892
893 **Processing and analysis of publicly available bulk gene expression data**
894 FASTQ files from a previously published analysis of peritoneal macrophages cultured under neutral pH
895 7.4 or acidic pH 6.8 conditions were downloaded from NCBI GEO (accession #GSE164697)[30]. FASTQ
896 files from a previously published analysis of peritoneal macrophages from WT or BMAL1 KO mice were
897 downloaded from EMBL- European Bioinformatics Institute Array Express (accession #E-MTAB-8411)[44].
898 FASTQ files from a previously published analysis of bone marrow-derived macrophages were
899 downloaded from NCBI GEO (accession #GSE157878)[77]. FASTQ files from a previously published
900 analysis of macrophages from tumor and tumor-adjacent tissue from NSCLC patients were downloaded
901 from NCBI GEO (accession #GSE116946) [104]. FASTQ files from a previous published study of tumor-
902 associated macrophages were downloaded from NCBI GEO (accession #GSE188549)[101]. Where
903 applicable, multiple FASTQ files of the same run were concatenated before processing and mapping. CEL
904 files from a previously published microarray time series analysis of peritoneal macrophages from WT
905 mice were downloaded from NCBI GEO (accession #GSE25585)[36]. CEL files from a previously published
906 microarray analysis of alveolar macrophages from healthy human donors were downloaded from NCBI
907 GEO (accession #GSE13896)[105].

All FASTQ files were processed with FASTP using default parameters to trim adaptors and remove reads that were low quality or too short[144]. Cleaned FASTQ files from mouse data were mapped to transcripts using Salmon 1.3.0 in mapping-based mode using a decoy-aware transcription built from the Gencode M27 GRCm39 primary assembly mouse genome and M27 mouse transcriptome, and from human data were mapped to transcripts using Salmon 1.4.0 in mapping-based mode using a decoy-aware transcription built from the Gencode v43 GRCh38 primary assembly human genome and v43 human transcriptome [145]. Single-end mapping was used for GSE188549, GSE116946 samples and paired-end mapping was used for E-MTAB-8411 and GSE164697. All transcripts were then collapsed to gene-level using Tximport v1.14.2 with the Gencode M27 transcriptome for mouse and the v43 transcriptome for human, and genes were annotated with symbols using the Ensembl GRCm39.104 transcriptome annotations for mouse and Ensembl GRCh38.111 transcriptome annotations for human [146]. Transcripts per million (TPM) outputted from Tximport were used for downstream analyses. Microarray data was imported and analyzed from CEL files using the packages affy and Limma, and genes were annotated with symbols using the University of Michigan Brain Array Custom CDF v25.0 for the Mouse Gene 1.0 ST Array or Human Gene 133 plus 2 Array[147, 148].

Clock correlation distance (CCD) analysis was performed as previously described[102]. Briefly, the default universal 12-gene molecular circadian clock reference correlation was used. Genes outside this 12-gene reference that were of zero variance across at least one of the sample groups were discarded prior to analysis. For delta CCD, which directly compares between each group, the sample group with the lowest CCD score (corresponding to the most ordered clock) was set as the control group, and $p<0.05$ was deemed significantly different from the control group.

WCGNA analysis to determine significant co-variance between pairs of clock genes was performed as previously described, using an expanded list of core circadian clock genes[101]. Results were calculated from Pearson correlations of log-transformed TPM values. For data presented in Figure 6, the gene-specific mean for TAMs within each group in the original publication (MHCII-high and MHCII-low, [101]) were subtracted out prior to analysis. Significance was determined by $p<0.05$ (Figure 6) or $p<0.01$ (Figure 7, Supplementary Figure 9).

Processing and analysis of publicly available single-cell gene expression data

A merged Seurat Object of single-cell RNA-sequencing data of immune cells infiltrating B16-F10 melanoma was downloaded from NCBI GEO (accession #GSE260641)[107]. Data were analyzed using Seurat 5.0.3[149]. Macrophages, which were previously annotated, were isolated, gene expression normalized, and the following factors regressed out: cell cycle state, mitochondrial content, and circadian timepoint. 9 clusters were identified with the FindNeighbors and FindClusters commands. UMAP was used to visualize macrophage clusters[150]. *Crem* high groups were identified from violin plot and confirmed with differential expression compared to *Crem* low groups. All differential expression was performed using the FindMarkers command only considering genes expressed within at least 10% of the comparison populations and with a minimum log fold change of 0.25 between populations (min.pct = 0.1 and logfc.theshold = 0.25). Significantly differentially expressed genes were determined by adjusted $p(adj.p)<0.05$ by the limma implementation of the Wilcoxon Rank Sum test (test.use = "wilcox_limma")[147, 151]. A differentially expressed genes shown are $p(adj.p)<0.005$.

Data sharing

All raw data, analyses, and code used for analyses are available at FigShare at the following link:

955 https://rochester.figshare.com/projects/Source_data_for_Circadian_rhythms_of_macrophages_are_alte

956 red_by_the_acidic_pH_of_the_tumor_microenvironment/210625

957

958 Acknowledgements

959 We would like to thank Dr. Jim Miller (Department of Microbiology and Immunology, University of

960 Rochester) and Dr. Paul Brookes (Department of Anesthesiology and Perioperative Medicine, University

961 of Rochester) for their intellectual contributions. We also thank Dr. Christoph Scheiermann (University of

962 Geneva, Geneva, Switzerland) for assistance with scRNA-seq data, and the University of Rochester

963 Genomics Research Center (GRC) with assistance with data analysis and preparation. All visual

964 illustrations were made using BioRender. The project described was supported by Grant Number

965 T32AI007285 (to AMKC) from the National Institute of Allergy and Infectious Diseases of the National

966 Institutes of Health (NIH), Grant Number T32GM135134 (to AMKC) from the National Institute of

967 General Medical Sciences of the National Institutes of Health, Grant Numbers R00CA204593 and

968 R01CA282225 (to BJA) from the National Cancer Institute of the National Institutes of Health, the

969 University of Rochester University Research Award (to BJA), and the Wilmot Predoctoral Cancer Research

970 Fellowship (to AMKC) from the Wilmot Cancer Institute at the University of Rochester. The contents of

971 this paper are solely the responsibility of the Authors and do not necessarily represent the official views

972 of the NIH.

973

974 Author Contributions

975 Conceptualization: Amelia M. Knudsen-Clark, Brian J. Altman

976 Data Curation: Amelia M. Knudsen-Clark, Cameron Baker, Matthew M. McCall, Brian J. Altman

977 Formal analysis: Amelia M. Knudsen-Clark, Kristina Morris, Cameron Baker, Matthew M. McCall, Lauren

978 M. Hablitz, Brian J. Altman

Funding acquisition: Amelia M. Knudsen-Clark, Brian J. Altman

Investigation: Amelia M. Knudsen-Clark, Daniel Mwangi, Juliana Cazarin

Methodology: Amelia M. Knudsen-Clark, Kristina Morris, Minsoo Kim, Brian J. Altman

Resources: Brian J. Altman

Software: Amelia M. Knudsen-Clark, Daniel Mwangi, Kristina Morris, Cameron Baker, Matthew M. McCall, Brian J. Altman

Supervision: Brian J. Altman

Validation: Amelia M. Knudsen-Clark

Visualization: Amelia M. Knudsen-Clark, Cameron Baker, Brian J. Altman

Writing – original draft: Amelia M. Knudsen-Clark

Writing – review and editing: Amelia M. Knudsen-Clark, Daniel Mwangi, Juliana Cazarin, Lauren M. Hablitz, Minsoo Kim, Brian J. Altman

Conflict of Interest

The authors declare no conflict of interest.

Figure Legends

Figure 1. Macrophages of different phenotypes have distinct circadian rhythms. Bone marrow-derived macrophages (BMDMs) were obtained from C57BL/6 mice expressing PER2-Luc. The circadian clocks of BMDMs were synchronized by a 24-hour period of serum starvation in media with 0% serum, followed by a 2-hour period of serum shock in media with 50% serum. Luciferase activity of BMDMs stimulated with either 10 ng/mL IL-4 and 10 ng/mL IL-13, or 50 ng/mL IFNγ and 100 ng/mL LPS; or left unstimulated was monitored in real time by LumiCycle. Data was baseline-subtracted using the running average.

Oscillation parameters of BMDMs were measured by LumiCycle Analysis. Shown are mean and standard error of the mean (SEM), n=5 biological replicates. Statistical significance determined by unpaired two-tailed t-test with Welch's correction; *, $p < 0.05$; **, $p<0.005$; ***, $p<0.0005$. Data shown are representative of 2 independent experiments.

Figure 2. Acidic pH alters circadian rhythms of bone marrow-derived macrophages *in vitro*. A-F. Bone marrow-derived macrophages (BMDMs) were obtained from C57BL/6 mice expressing PER2-Luc. The circadian clocks of BMDMs were synchronized by a 24-hour period of serum starvation in media with 0% serum, followed by a 2-hour period of serum shock in media with 50% serum. BMDMs were then cultured in media with neutral pH 7.4 or acidic media with pH 6.8 or 6.5, and stimulated with either (**B,E**) 10 ng/mL IL-4 and 10 ng/mL IL-13, or (**C,F**) 50 ng/mL IFNγ and 100 ng/mL LPS; or (**A,D**) left unstimulated. **A-C**. Luciferase activity was monitored in real time by LumiCycle. Shown are mean and SEM, n=2 biological replicates, representative of 2 independent experiments. Data from both experiments was baseline-subtracted using the running average, and oscillation parameters were measured by LumiCycle Analysis. Shown are mean and SEM, n=5 biological replicates. **D-F**. In parallel, RNA was collected at 12, 16, 20, and 24 hours post-synchronization, and qt-PCR was performed to assess oscillation of transcripts encoding core clock proteins in macrophages under acidic conditions. Shown are mean and SEM, n=3 biological replicates. Data shown are representative of 2 independent experiments. Statistical significance determined by unpaired two-tailed t-test with Welch's correction; *, $p < 0.05$; **, $p<0.005$; ***, $p<0.0005$.

Figure 3. Acidic pH alters circadian rhythms of peritoneal macrophages *ex vivo* at temporally distinct times of day. A,C. Peritoneal macrophages were obtained at ZT0 or ZT12 from C57BL/6 mice expressing PER2-Luc and cultured in media with neutral pH 7.4 or acidic pH 6.5. **A**. Luciferase activity was monitored

in real time by LumiCycle. Data was baseline-subtracted using the running average; shown is the mean and SEM, n=2, representative of 2 independent experiments. Oscillation parameters were measured by LumiCycle Analysis; shown is the mean and SEM, n=4, data pooled from 2 independent experiments. **B**. Clock gene expression, in transcripts per million (TPM), of peritoneal macrophages cultured in media at pH 7.4 or pH 6.8 for 24 hours, sourced from publicly available data (see **Methods**) shown is mean and SEM, n=3. **C**. The magnitude of change in circadian oscillation parameters between macrophages at pH 7.4 and pH 6.5 was compared between peritoneal macrophages taken at ZT 0 or ZT 12. Shown is the mean and SEM, n=4; data pooled from 2 independent experiments. Statistical significance determined by paired two-tailed t-test with Welch's correction; *, $p < 0.05$; **, $p<0.005$; ***, $p<0.0005$.

Figure 4. Lactate alters circadian rhythms in macrophages, both alone and in conjunction with acidic pH. A-C. Bone marrow-derived macrophages (BMDMs) were obtained from C57BL/6 mice expressing PER2-Luc. The circadian clocks of BMDMs were synchronized by a 24-hour period of serum starvation in media with 0% serum, followed by a 2-hour period of serum shock in media with 50% serum. BMDMs were then cultured in media with neutral pH 7.4 or acidic pH 6.5, supplemented with 0 mM or 25 mM sodium-L-lactate. **A**. RNA was collected at 6 hours post-treatment, and expression of pro-resolution phenotype markers *Arg1* or *Vegf* was quantified by qt-PCR. Shown is the mean and SEM, n=6, data pooled from 2 independent experiments. **B**. Luciferase activity was monitored in real time by LumiCycle. Shown is the mean and SEM, n=4; data representative of 2 independent experiments. Data was baseline-subtracted using the running average, and oscillation parameters were measured by LumiCycle Analysis. Shown is the mean and SEM, n=7-10; data pooled from 2 independent experiments. **C**. RNA was collected at 12, 16, 20, and 24 hours post-synchronization, and qt-PCR was performed to assess oscillation of transcripts encoding core clock proteins in macrophages exposed to lactate. Shown is the mean and SEM, n=5-6; data pooled from 2 independent experiments. Statistical significance determined

by unpaired two-tailed t-test with Welch's correction; *, $p < 0.05$; **, $p<0.005$; ***, $p<0.0005$; ****, $p<0.00005$.

Figure 5. pH-induced changes in circadian rhythms are not driven by cAMP signaling alone. A-B. Bone marrow-derived macrophages (BMDMs) were obtained from C57BL/6 mice expressing PER2-Luc. BMDMs were cultured in media with neutral pH 7.4 or acidic pH 6.5, and (**A**) treated with vehicle or 20, 40 or 80 uM Forsokolin, or (**B**) treated with vehicle or 20, 40, 80 uM IBMX. Luciferase activity was monitored in real time by LumiCycle. Data was baseline-subtracted using the running average. Shown is the mean, n=2. **C.** The circadian clocks of BMDMs were synchronized by a 24-hour period of serum starvation in media with 0% serum, followed by a 2-hour period of serum shock in media with 50% serum. BMDMs were then cultured in media with neutral pH 7.4 or acidic pH 6.5, and treated with vehicle or 5, 10, or 15uM MDL-12330A (MDL-12). Luciferase activity was monitored in real time by LumiCycle. Data was baseline-subtracted using the running average, and oscillation parameters were measured by LumiCycle Analysis. Shown is the mean and SEM, n=4. **D.** Expression of genes associated with acid sensing (*Icer*) and pro-resolution phenotype (*Arg1*) was measured at 2 hours post-treatment (CT2). Shown is the mean and SEM; n=3. **E.** Phosphorylation of CREB was assessed by immunoblot at the indicated timepoints after synchronization, MDL-12 treatment, and exposure to low pH. **F.** Relative pCREB levels from (**E**) were quantified; band intensity was normalized to total protein, n=3. Statistical significance determined by unpaired two-tailed t-test with Welch's correction; *, $p < 0.05$; **, $p<0.005$; ***, $p<0.0005$; ****, $p<0.00005$. Data shown are representative of 2-3 independent experiments.

Figure 6. Clock correlation distance (CCD) and weighted gene co-expression network analysis (WGCNA) provides evidence of circadian disorder in murine tumor-associated macrophages. A. RNA-seq datasets (see **Methods**) of WT peritoneal macrophages, BMAL1 KO peritoneal macrophages, and tumor-

associated macrophages (TAMs) were analyzed for expression of *Arg1* and *Crem*. **B.** A pan-tissue murine reference control was used for clock correlation distance (CCD). **C-D.** (**C**) Clock correlation distance (CCD) analysis was performed and (**D**) statistical analysis to compare CCD scores was performed by calculating delta CCD, with $p<0.05$ being deemed significantly different from the control group. **E**. Weighted gene co-expression network analysis (WGCNA) was performed on the indicated circadian clock genes using data from (**A-D**); asterisks represent significant covariance, where $p< 0.05$.

Figure 7. Clock correlation distance (CCD) and weighted gene co-expression network analysis (WGCNA) provides evidence of circadian disorder in human tumor-associated macrophages. A. Clock correlation distance (CCD) analysis was performed using RNA-seq datasets of macrophages from tumor (TAMs) and tumor-adjacent tissue from NSCLC patients and alveolar macrophages from healthy donors (see **Methods**). TAM samples were subset by median *Crem* expression into *Crem* high TAM samples (TAMs *Crem* high) and *Crem* low TAM samples (TAMs *Crem* low). **B.** Statistical analysis to compare CCD scores was performed by calculating delta CCD, with $p<0.05$ being deemed significantly different from the control group. **C.** Weighted gene co-expression network analysis (WGCNA) was performed on the indicated circadian clock genes using data from (**A-B**); asterisks represent significant covariance, where $p< 0.01$.

Figure 8. Heterogeneity in circadian rhythms of cells within a population can lead to circadian disorder observed by CCD. A-C. Increasingly desynchronized populations were modeled using an microarray data set of WT peritoneal macrophages (n=12) taken at 4-hour intervals across two days (see **Methods**). **A.** A schematic of the populations used in experimental design. **B-C.** (**B**) Clock correlation distance (CCD) analysis was performed and (**C**) statistical analysis to compare CCD scores was performed by calculating delta CCD, with $p<0.05$ being deemed significantly different from the control group.

Figure 9. There is heterogeneity in expression of circadian clock genes within the tumor-associated macrophage population. We analyzed a single-cell RNA-seq dataset of tumor-associated macrophages. **A.** Unbiased clustering was performed to identify TAM subpopulations. **B.** Differential gene expression analysis was performed on these TAM clusters, and expression of significantly different circadian genes was plotted along with *Crem*. **C.** Crem expression of macrophages in TAM clusters was measured. **D.** TAMs were subset by *Crem* expression into *Crem* high TAMs and *Crem* low TAMs, and these groups were overlaid on the UMAP plot shown in (**A**). **E.** Differential gene expression analysis was performed on *Crem* high vs *Crem* low, and expression of significantly different circadian genes was plotted. All differentially expressed genes or groups of clusters in (**B**), (**C**), and (**E**) are adj.p<0.005 by limma implementation of the Wilcoxon Rank Sum test.

Figure 10. A functional circadian clock in macrophages can influence tumor growth in a murine model of PDAC. Bone marrow-derived macrophages (BMDMs) obtained from WT or BMAL1 KO mice were subcutaneously co-injected with KCKO cells into the flank of WT mice. Tumor growth was measured by caliper. Shown is the mean and SEM; n=20 individual mice, 10 male and 10 female. Statistical significance determined at each time point by unpaired two-tailed t-test with Welch's correction; *, $p < 0.05$; **, p<0.005; ***, p<0.0005. Data shown are representative of 2 independent experiments.

Supplementary Figure 1. Polarization of macrophages toward pro-resolution or pro-inflammatory phenotype. Bone marrow-derived macrophages (BMDMs) were derived from C57BL/6 mice expressing PER2-Luc. The circadian clocks of BMDMs were synchronized by a 24-hour period of serum starvation in media with 0% serum, followed by a 2-hour period of serum shock in media with 50% serum. BMDMs were then stimulated with either 10 ng/mL IL-4 and 10 ng/mL IL-13, or 50 ng/mL IFNγ and 100 ng/mL

LPS; or left unstimulated. RNA was collected at 6 hours post-synchronization, and qt-PCR was performed to assess expression of phenotype-associated genes. Shown are mean and standard error of the mean (SEM), n=3 biological replicates. Statistical significance determined by unpaired two-tailed t-test with Welch's correction; *, $p < 0.05$; **, ***, $p<0.0005$. Data shown are representative of 2 independent experiments.

Supplementary Figure 2. The PER2-Luciferase reporter system enables real-time monitoring of circadian rhythms of macrophages. A. A schematic of the PER2-Luciferase (PER2-Luc) luciferase reporter system. **B.** A schematic of the synchronization protocol in which the circadian clocks of bone marrow-derived macrophages (BMDMs) derived from C57BL/6 mice expressing PER2-Luc were synchronized by a 24-hour period of serum starvation in media with 0% serum, followed by a 2-hour period of serum shock in media with 50% serum. **C.** BMDMs were then cultured in RPMI/10% FBS supplemented with D-luciferin at circadian time (CT) 0. Luciferase activity of BMDMs was monitored in real time by LumiCycle. **D-E.** Protein and RNA were collected at the indicated times post-serum shock to assess (**D**) cAMP signaling by p-CREB levels a€(**E**) expression of *Icer*. Statistical significance determined by unpaired two-tailed t-test with Welch's correction; **, $p < 0.005$. Data shown are representative of 2 independent experiments.

Supplementary Figure 3. Macrophages sense and respond to an acidic extracellular environment when cultured *in vitro* in media with acidic pH. A-B. Bone marrow-derived macrophages (BMDMs) were obtained from C57BL/6 mice expressing PER2-Luc. BMDMs were cultured in media with pH 7.4 or acidic media with pH 6.5, and stimulated with either 10 ng/mL IL-4 and 10 ng/mL IL-13, or 50 ng/mL IFNγ and 100 ng/mL LPS; or left unstimulated. RNA was collected at 2 hours post-treatment, and qt-PCR was performed to assess expression of genes associated with (**A**) phenotype or (**B**) acid sensing in

macrophages. Shown are mean and SEM, n=3 biological replicates. Statistical significance determined by two-tailed t-test with Welch's correction; *, $p < 0.05$; **, $p<0.005$; ***, $p<0.0005$; ****, $p<0.00005$. Data shown are representative of 2 independent experiments.

Supplementary Figure 4. Survival of macrophages under acidic pH. A. Lumicycle data from **Figure 2-A-C** are presented as axis-matched graphs. **B.** Bone marrow-derived macrophages (BMDMs) were obtained from C57BL/6 mice expressing PER2-Luc. The circadian clocks of BMDMs were synchronized by a 24-hour period of serum starvation in media with 0% serum, followed by a 2-hour period of serum shock in media with 50% serum. BMDMs were then cultured in media with pH 7.4 or acidic media with pH 6.8 or 6.5, and stimulated with either 10 ng/mL IL-4 and 10 ng/mL IL-13, or 50 ng/mL IFNγ and 100 ng/mL LPS; or left unstimulated. Cells were fixed at CT 1, 2, and 3 days post-treatment and stained with DAPI. Number of nuclei was counted using Celigo to determine the number of adherent cells. **C.** Supernatant from (**A**) was collected at CT 12, 24, 36, and 48 hours and pH of media was measured. Shown is the mean and SEM, n=3. Statistical significance determined by multiple unpaired t-test with Welch's correction; *, $p < 0.05$; **, $p<0.005$; ***, $p<0.0005$. Data shown are representative of 2 independent experiments.

Supplementary Figure 5. Exposure to cancer cell supernatant further modulates circadian rhythms in addition to pH-driven changes. Bone marrow-derived macrophages (BMDMs) were obtained from C57BL/6 mice expressing PER2-Luc. The circadian clocks of BMDMs were synchronized by a 24-hour period of serum starvation in media with 0% serum, followed by a 2-hour period of serum shock in media with 50% serum. BMDMs were then cultured in RPMI with neutral pH 7.4 or acidic pH 6.5, or in KCKO supernatant at pH 6.5 or pH-adjusted to pH 7.4. Luciferase activity was monitored in real time by LumiCycle. Data was baseline-subtracted using the running average, and oscillation parameters were

measured by LumiCycle Analysis. Shown is the mean and SEM, n=4. Statistical significance determined by unpaired two-tailed t-test with Welch's correction; *, $p < 0.05$; **, $p<0.005$; ***, $p<0.0005$; ****, $p<0.00005$.

Supplementary Figure 6. Acidic pH alters circadian rhythms in macrophages in the absence of prior serum starvation followed by serum shock. Bone marrow-derived macrophages (BMDMs) were obtained from C57BL/6 mice expressing PER2-Luc. BMDMs were cultured in media with neutral pH 7.4 or acidic pH 6.8 or 6.5. Luciferase activity was monitored in real time by LumiCycle. Data was baseline-subtracted using the running average, and oscillation parameters were measured by LumiCycle Analysis. Shown is the mean and SEM, n=4-5. Data pooled from 2 individual experiments. Statistical significance determined by unpaired two-tailed t-test with Welch's correction; ***, $p<0.0005$; ****, $p<0.00005$.

Supplementary Figure 7. Pre-treatment with 15 uM MDL-12 for up to 2 hours is not necessary to suppress pH-driven changes in amplitude of circadian rhythms. A-E. Bone marrow-derived macrophages (BMDMs) were obtained from C57BL/6 mice expressing PER2-Luc. The circadian clocks of BMDMs were synchronized by a 24-hour period of serum starvation in media with 0% serum, followed by a 2-hour period of serum shock in media with 50% serum. (**A**) BMDMs were then cultured in media with neutral pH 7.4 or acidic pH 6.5, and treated with vehicle or 15uM MDL-12. Alternately, (**B,C**) BMDMs were cultured at pH 7.4 and pre-treated with 15uM MDL-12 for 30 minutes or (**D,E**) 2 hours, after which media was removed and cells were cultured in media at pH 7.4 or pH 6.5 in the (**C,E**) presence or (**B,D**) absence of MDL-12. Luciferase activity was monitored in real time by LumiCycle. Shown is the mean, n=2 biological replicates. Data for cells that received no pre-treatment (**A**) was overlaid on plots of data where cells received pre-treatment (**B-E**) to allow for comparison of changes in rhythms.

Supplementary Figure 8. Macrophages from BMAL1 KO mice have disrupted circadian rhythms. A. Levels of Bmal1 in bone marrow-derived macrophages (BMDMs) from WT or BMAL1 KO mice were assessed by immunoblot. **B.** To confirm functional disruption of the circadian clock, peritoneal macrophages or BMDMs were obtained from WT or BMAL1 KO mice expressing PER2-Luc and cultured *in vitro* with D-luciferin. Luciferase activity was monitored in real time by LumiCycle. Shown is the mean and SEM, n=2, representative of 2 independent experiments.

Supplementary Figure 9. Heterogeneity in circadian rhythms of cells within a population can lead to an altered circadian clock gene network in samples. Increasingly desynchronized populations were modeled using an RNA-seq data set of WT peritoneal macrophages taken at 4-hour intervals across two days (see **Methods**). Weighted gene co-expression network analysis (WGCNA) was performed; asterisks represent significant covariance, where $p < 0.01$.

References

1. Cassetta, L. and J.W. Pollard, *Targeting macrophages: therapeutic approaches in cancer.* Nat Rev Drug Discov, 2018. **17**(12): p. 887-904.
2. Zhang, Q.W., et al., *Prognostic significance of tumor-associated macrophages in solid tumor: a meta-analysis of the literature.* PLoS One, 2012. **7**(12): p. e50946.
3. Gentles, A.J., et al., *The prognostic landscape of genes and infiltrating immune cells across human cancers.* Nat Med, 2015. **21**(8): p. 938-945.
4. DeNardo, D.G. and B. Ruffell, *Macrophages as regulators of tumour immunity and immunotherapy.* Nat Rev Immunol, 2019.
5. Mosser, D.M. and J.P. Edwards, *Exploring the full spectrum of macrophage activation.* Nat Rev Immunol, 2008. **8**(12): p. 958-69.
6. Murray, P.J. and T.A. Wynn, *Protective and pathogenic functions of macrophage subsets.* Nat Rev Immunol, 2011. **11**(11): p. 723-37.
7. Coussens, L.M. and Z. Werb, *Inflammation and cancer.* Nature, 2002. **420**(6917): p. 860-7.
8. Murray, P.J., *Nonresolving macrophage-mediated inflammation in malignancy.* Febs j, 2018. **285**(4): p. 641-653.
9. Schoppmann, S.F., et al., *Tumor-associated macrophages express lymphatic endothelial growth factors and are related to peritumoral lymphangiogenesis.* Am J Pathol, 2002. **161**(3): p. 947-56.
10. Huber, R., et al., *Tumour hypoxia promotes melanoma growth and metastasis via High Mobility Group Box-1 and M2-like macrophages.* Sci Rep, 2016. **6**: p. 29914.
11. Graham, D.K., et al., *The TAM family: phosphatidylserine sensing receptor tyrosine kinases gone awry in cancer.* Nat Rev Cancer, 2014. **14**(12): p. 769-85.
12. Cook, R.S., et al., *MerTK inhibition in tumor leukocytes decreases tumor growth and metastasis.* J Clin Invest, 2013. **123**(8): p. 3231-42.
13. Roberts, A.W., et al., *Tissue-Resident Macrophages Are Locally Programmed for Silent Clearance of Apoptotic Cells.* Immunity, 2017. **47**(5): p. 913-927.e6.
14. Fadok, V.A., et al., *Macrophages that have ingested apoptotic cells in vitro inhibit proinflammatory cytokine production through autocrine/paracrine mechanisms involving TGF-beta, PGE2, and PAF.* J Clin Invest, 1998. **101**(4): p. 890-8.
15. Strassmann, G., et al., *Evidence for the involvement of interleukin 10 in the differential deactivation of murine peritoneal macrophages by prostaglandin E2.* J Exp Med, 1994. **180**(6): p. 2365-70.
16. Kuang, D.M., et al., *Activated monocytes in peritumoral stroma of hepatocellular carcinoma foster immune privilege and disease progression through PD-L1.* J Exp Med, 2009. **206**(6): p. 1327-37.
17. Ruffell, B. and L.M. Coussens, *Macrophages and therapeutic resistance in cancer.* Cancer Cell, 2015. **27**(4): p. 462-72.
18. Mantovani, A., et al., *Macrophages as tools and targets in cancer therapy.* Nature Reviews Drug Discovery, 2022. **21**(11): p. 799-820.
19. Cuccarese, M.F., et al., *Heterogeneity of macrophage infiltration and therapeutic response in lung carcinoma revealed by 3D organ imaging.* Nat Commun, 2017. **8**: p. 14293.
20. Chevrier, S., et al., *An Immune Atlas of Clear Cell Renal Cell Carcinoma.* Cell, 2017. **169**(4): p. 736-749.e18.

21. Laviron, M., et al., *Tumor-associated macrophage heterogeneity is driven by tissue territories in breast cancer.* Cell Rep, 2022. **39**(8): p. 110865.
22. Nalio Ramos, R., et al., *Tissue-resident FOLR2(+) macrophages associate with CD8(+) T cell infiltration in human breast cancer.* Cell, 2022. **185**(7): p. 1189-1207.e25.
23. Yano, S., et al., *Spatial-temporal FUCCI imaging of each cell in a tumor demonstrates locational dependence of cell cycle dynamics and chemoresponsiveness.* Cell Cycle, 2014. **13**(13): p. 2110-9.
24. Huang, Y.K., et al., *Macrophage spatial heterogeneity in gastric cancer defined by multiplex immunohistochemistry.* Nat Commun, 2019. **10**(1): p. 3928.
25. Lyssiotis, C.A. and A.C. Kimmelman, *Metabolic Interactions in the Tumor Microenvironment.* Trends Cell Biol, 2017. **27**(11): p. 863-875.
26. Raghunand, N., R.A. Gatenby, and R.J. Gillies, *Microenvironmental and cellular consequences of altered blood flow in tumours.* Br J Radiol, 2003. **76 Spec No 1**: p. S11-22.
27. Gillies, R.J., et al., *Targeting acidity in cancer and diabetes.* Biochim Biophys Acta Rev Cancer, 2019. **1871**(2): p. 273-280.
28. El-Kenawi, A., et al., *Acidity promotes tumour progression by altering macrophage phenotype in prostate cancer.* Br J Cancer, 2019. **121**(7): p. 556-566.
29. Bohn, T., et al., *Tumor immunoevasion via acidosis-dependent induction of regulatory tumor-associated macrophages.* Nat Immunol, 2018. **19**(12): p. 1319-1329.
30. Jiang, W., et al., *Extracellular Acidity Reprograms Macrophage Metabolism and Innate Responsiveness.* The Journal of Immunology, 2021. **206**(12): p. 3021-3031.
31. Partch, C.L., C.B. Green, and J.S. Takahashi, *Molecular architecture of the mammalian circadian clock.* Trends Cell Biol, 2014. **24**(2): p. 90-9.
32. Walton, Z.E., et al., *Acid Suspends the Circadian Clock in Hypoxia through Inhibition of mTOR.* Cell, 2018. **174**(1): p. 72-87.e32.
33. Mure, L.S., et al., *Diurnal transcriptome atlas of a primate across major neural and peripheral tissues.* Science, 2018. **359**(6381).
34. Zhang, R., et al., *A circadian gene expression atlas in mammals: implications for biology and medicine.* Proc Natl Acad Sci U S A, 2014. **111**(45): p. 16219-24.
35. Haspel, J.A., et al., *Perfect timing: circadian rhythms, sleep, and immunity - an NIH workshop summary.* JCI Insight, 2020. **5**(1).
36. Keller, M., et al., *A circadian clock in macrophages controls inflammatory immune responses.* Proc Natl Acad Sci U S A, 2009. **106**(50): p. 21407-12.
37. Silver, A.C., et al., *Circadian expression of clock genes in mouse macrophages, dendritic cells, and B cells.* Brain Behav Immun, 2012. **26**(3): p. 407-13.
38. Nguyen, K.D., et al., *Circadian gene Bmal1 regulates diurnal oscillations of Ly6C(hi) inflammatory monocytes.* Science, 2013. **341**(6153): p. 1483-8.
39. Baumann, A., et al., *The circadian clock is functional in eosinophils and mast cells.* Immunology, 2013. **140**(4): p. 465-74.
40. Adrover, J.M., et al., *A Neutrophil Timer Coordinates Immune Defense and Vascular Protection.* Immunity, 2019. **50**(2): p. 390-402.e10.
41. Arjona, A. and D.K. Sarkar, *Circadian oscillations of clock genes, cytolytic factors, and cytokines in rat NK cells.* J Immunol, 2005. **174**(12): p. 7618-24.
42. Druzd, D., et al., *Lymphocyte Circadian Clocks Control Lymph Node Trafficking and Adaptive Immune Responses.* Immunity, 2017. **46**(1): p. 120-132.
43. Scheiermann, C., et al., *Clocking in to immunity.* Nat Rev Immunol, 2018. **18**(7): p. 423-437.
44. Kitchen, G.B., et al., *The clock gene Bmal1 inhibits macrophage motility, phagocytosis, and impairs defense against pneumonia.* Proc Natl Acad Sci U S A, 2020.

45. Gibbs, J.E., et al., *The nuclear receptor REV-ERBalpha mediates circadian regulation of innate immunity through selective regulation of inflammatory cytokines.* Proc Natl Acad Sci U S A, 2012. **109**(2): p. 582-7.
46. He, W., et al., *Circadian Expression of Migratory Factors Establishes Lineage-Specific Signatures that Guide the Homing of Leukocyte Subsets to Tissues.* Immunity, 2018. **49**(6): p. 1175-1190.e7.
47. Nobis, C.C., et al., *The circadian clock of CD8 T cells modulates their early response to vaccination and the rhythmicity of related signaling pathways.* Proc Natl Acad Sci U S A, 2019. **116**(40): p. 20077-20086.
48. Fortier, E.E., et al., *Circadian variation of the response of T cells to antigen.* J Immunol, 2011. **187**(12): p. 6291-300.
49. Beam, C.A., et al., *Synchronization of the Normal Human Peripheral Immune System: A Comprehensive Circadian Systems Immunology Analysis.* Sci Rep, 2020. **10**(1): p. 672.
50. Mazzoccoli, G., et al., *A timetable of 24-hour patterns for human lymphocyte subpopulations.* J Biol Regul Homeost Agents, 2011. **25**(3): p. 387-95.
51. Silver, A.C., et al., *The circadian clock controls toll-like receptor 9-mediated innate and adaptive immunity.* Immunity, 2012. **36**(2): p. 251-61.
52. Phillips, A.C., et al., *Preliminary evidence that morning vaccination is associated with an enhanced antibody response in men.* Psychophysiology, 2008. **45**(4): p. 663-6.
53. Long, J.E., et al., *Morning vaccination enhances antibody response over afternoon vaccination: A cluster-randomised trial.* Vaccine, 2016. **34**(24): p. 2679-85.
54. Curtis, A.M., et al., *Circadian control of innate immunity in macrophages by miR-155 targeting Bmal1.* Proc Natl Acad Sci U S A, 2015. **112**(23): p. 7231-6.
55. Deng, W., et al., *The Circadian Clock Controls Immune Checkpoint Pathway in Sepsis.* Cell Rep, 2018. **24**(2): p. 366-378.
56. Aiello, I., et al., *Circadian disruption promotes tumor-immune microenvironment remodeling favoring tumor cell proliferation.* Sci Adv, 2020. **6**(42).
57. Tsuruta, A., et al., *Diurnal Expression of PD-1 on Tumor-Associated Macrophages Underlies the Dosing Time-Dependent Antitumor Effects of the PD-1/PD-L1 Inhibitor BMS-1 in B16/BL6 Melanoma-Bearing Mice.* Mol Cancer Res, 2022. **20**(6): p. 972-982.
58. Strauss, L., et al., *Targeted deletion of PD-1 in myeloid cells induces antitumor immunity.* Sci Immunol, 2020. **5**(43).
59. Qian, D.C., et al., *Effect of immunotherapy time-of-day infusion on overall survival among patients with advanced melanoma in the USA (MEMOIR): a propensity score-matched analysis of a single-centre, longitudinal study.* Lancet Oncol, 2021. **22**(12): p. 1777-1786.
60. Munder, M., K. Eichmann, and M. Modolell, *Alternative metabolic states in murine macrophages reflected by the nitric oxide synthase/arginase balance: competitive regulation by CD4+ T cells correlates with Th1/Th2 phenotype.* J Immunol, 1998. **160**(11): p. 5347-54.
61. Murray, P.J., *Macrophage Polarization.* Annual Review of Physiology, 2017. **79**(Volume 79, 2017): p. 541-566.
62. Biswas, S.K. and A. Mantovani, *Macrophage plasticity and interaction with lymphocyte subsets: cancer as a paradigm.* Nat Immunol, 2010. **11**(10): p. 889-96.
63. Viola, A., et al., *The Metabolic Signature of Macrophage Responses.* Front Immunol, 2019. **10**: p. 1462.
64. Nathan, C.F., et al., *Identification of interferon-gamma as the lymphokine that activates human macrophage oxidative metabolism and antimicrobial activity.* J Exp Med, 1983. **158**(3): p. 670-89.
65. Hörhold, F., et al., *Reprogramming of macrophages employing gene regulatory and metabolic network models.* PLOS Computational Biology, 2020. **16**(2): p. e1007657.

66. Mills, C.D., et al., *M-1/M-2 macrophages and the Th1/Th2 paradigm.* J Immunol, 2000. **164**(12): p. 6166-73.
67. Stein, M., et al., *Interleukin 4 potently enhances murine macrophage mannose receptor activity: a marker of alternative immunologic macrophage activation.* J Exp Med, 1992. **176**(1): p. 287-92.
68. Allen, J.E., *IL-4 and IL-13: Regulators and Effectors of Wound Repair.* Annu Rev Immunol, 2023. **41**: p. 229-254.
69. Mantovani, A., et al., *Macrophage plasticity and polarization in tissue repair and remodelling.* J Pathol, 2013. **229**(2): p. 176-85.
70. Pesce, J.T., et al., *Retnla (relmalpha/fizz1) suppresses helminth-induced Th2-type immunity.* PLoS Pathog, 2009. **5**(4): p. e1000393.
71. McWhorter, F.Y., et al., *Modulation of macrophage phenotype by cell shape.* Proc Natl Acad Sci U S A, 2013. **110**(43): p. 17253-8.
72. Biswas, S.K., et al., *A distinct and unique transcriptional program expressed by tumor-associated macrophages (defective NF-kappaB and enhanced IRF-3/STAT1 activation).* Blood, 2006. **107**(5): p. 2112-22.
73. Ding, C., et al., *Tumor Microenvironment Modulates Immunological Outcomes of Myeloid Cells with mTORC1 Disruption.* J Immunol, 2019. **202**(5): p. 1623-1634.
74. Martinez, F.O. and S. Gordon, *The M1 and M2 paradigm of macrophage activation: time for reassessment.* F1000Prime Rep, 2014. **6**: p. 13.
75. Binger, K.J., et al., *High salt reduces the activation of IL-4– and IL-13–stimulated macrophages.* The Journal of Clinical Investigation, 2015. **125**(11): p. 4223-4238.
76. Yoo, S.H., et al., *PERIOD2::LUCIFERASE real-time reporting of circadian dynamics reveals persistent circadian oscillations in mouse peripheral tissues.* Proc Natl Acad Sci U S A, 2004. **101**(15): p. 5339-46.
77. Collins, E.J., et al., *Post-transcriptional circadian regulation in macrophages organizes temporally distinct immunometabolic states.* Genome Res, 2021. **31**(2): p. 171-85.
78. Rodheim, K., C. Jung, and K. Wright, *016 Associations between Circadian Melatonin and Temperature Amplitudes during Constant Routine.* Sleep, 2021. **44**(Supplement_2): p. A8-A8.
79. Wu, G., et al., *Normalized coefficient of variation (nCV): a method to evaluate circadian clock robustness in population scale data.* Bioinformatics, 2021. **37**(23): p. 4581-4583.
80. Chen, S., et al., *A Pro- and Anti-inflammatory Axis Modulates the Macrophage Circadian Clock.* Front Immunol, 2020. **11**: p. 867.
81. Lellupitiyage Don, S.S., et al., *Macrophage circadian rhythms are differentially affected based on stimuli.* Integr Biol (Camb), 2022. **14**(3): p. 62-75.
82. Pilorz, V., et al., *A Novel Mechanism Controlling Resetting Speed of the Circadian Clock to Environmental Stimuli.* Current Biology, 2014. **24**(7): p. 766-773.
83. Abe, M., et al., *Circadian rhythms in isolated brain regions.* J Neurosci, 2002. **22**(1): p. 350-6.
84. Gaspar, L.S., et al., *The importance of determining circadian parameters in pharmacological studies.* British Journal of Pharmacology, 2019. **176**(16): p. 2827-2847.
85. Boedtkjer, E. and S.F. Pedersen, *The Acidic Tumor Microenvironment as a Driver of Cancer.* Annual Review of Physiology, 2020. **82**(1): p. 103-126.
86. Gillies, R.J., Z. Liu, and Z. Bhujwalla, *31P-MRS measurements of extracellular pH of tumors using 3-aminopropylphosphonate.* Am J Physiol, 1994. **267**(1 Pt 1): p. C195-203.
87. Estrella, V., et al., *Acidity Generated by the Tumor Microenvironment Drives Local Invasion.* Cancer Research, 2013. **73**(5): p. 1524-1535.
88. Lv, S., et al., *A negative feedback loop of ICER and NF-κB regulates TLR signaling in innate immune responses.* Cell Death Differ, 2017. **24**(3): p. 492-499.
89. Kraut, J.A. and N.E. Madias, *Lactic acidosis.* N Engl J Med, 2014. **371**(24): p. 2309-19.

90. Pastorekova, S. and R.J. Gillies, *The role of carbonic anhydrase IX in cancer development: links to hypoxia, acidosis, and beyond.* Cancer Metastasis Rev, 2019. **38**(1-2): p. 65-77.
91. Swietach, P., *What is pH regulation, and why do cancer cells need it?* Cancer Metastasis Rev, 2019. **38**(1-2): p. 5-15.
92. de la Cruz-López, K.G., et al., *Lactate in the Regulation of Tumor Microenvironment and Therapeutic Approaches.* Front Oncol, 2019. **9**: p. 1143.
93. Colegio, O.R., et al., *Functional polarization of tumour-associated macrophages by tumour-derived lactic acid.* Nature, 2014. **513**(7519): p. 559-63.
94. Kidiyoor, A., et al., *Pancreatic Cancer Cells Isolated from Muc1-Null Tumors Favor the Generation of a Mature Less Suppressive MDSC Population.* Front Immunol, 2014. **5**: p. 67.
95. Besmer, D.M., et al., *Pancreatic ductal adenocarcinoma mice lacking mucin 1 have a profound defect in tumor growth and metastasis.* Cancer Res, 2011. **71**(13): p. 4432-42.
96. Polumuri, S., D.J. Perkins, and S.N. Vogel, *cAMP levels regulate macrophage alternative activation marker expression.* Innate Immun, 2021. **27**(2): p. 133-142.
97. Tavares, L.P., et al., *Blame the signaling: Role of cAMP for the resolution of inflammation.* Pharmacol Res, 2020. **159**: p. 105030.
98. Yagita, K. and H. Okamura, *Forskolin induces circadian gene expression of rPer1, rPer2 and dbp in mammalian rat-1 fibroblasts.* FEBS Lett, 2000. **465**(1): p. 79-82.
99. O'Neill, J.S., et al., *cAMP-dependent signaling as a core component of the mammalian circadian pacemaker.* Science, 2008. **320**(5878): p. 949-53.
100. Misra, U.K. and S.V. Pizzo, *Coordinate regulation of forskolin-induced cellular proliferation in macrophages by protein kinase A/cAMP-response element-binding protein (CREB) and Epac1-Rap1 signaling: effects of silencing CREB gene expression on Akt activation.* J Biol Chem, 2005. **280**(46): p. 38276-89.
101. Geeraerts, X., et al., *Macrophages are metabolically heterogeneous within the tumor microenvironment.* Cell Rep, 2021. **37**(13): p. 110171.
102. Shilts, J., G. Chen, and J.J. Hughey, *Evidence for widespread dysregulation of circadian clock progression in human cancer.* PeerJ, 2018. **6**: p. e4327.
103. Chun, S.K., et al., *Disruption of the circadian clock drives Apc loss of heterozygosity to accelerate colorectal cancer.* Sci Adv, 2022. **8**(32): p. eabo2389.
104. Garrido-Martin, E.M., et al., *M1(hot) tumor-associated macrophages boost tissue-resident memory T cells infiltration and survival in human lung cancer.* J Immunother Cancer, 2020. **8**(2).
105. Shaykhiev, R., et al., *Smoking-dependent reprogramming of alveolar macrophage polarization: implication for pathogenesis of chronic obstructive pulmonary disease.* J Immunol, 2009. **183**(4): p. 2867-83.
106. Pariollaud, M., et al., *Circadian disruption enhances HSF1 signaling and tumorigenesis in Kras-driven lung cancer.* Science Advances, 2022. **8**(39): p. eabo1123.
107. Wang, C., et al., *Circadian tumor infiltration and function of CD8+ T cells dictate immunotherapy efficacy.* Cell, 2024. **187**(11): p. 2690-2702.e17.
108. Mills, B.N., et al., *Stereotactic Body Radiation and Interleukin-12 Combination Therapy Eradicates Pancreatic Tumors by Repolarizing the Immune Microenvironment.* Cell Rep, 2019. **29**(2): p. 406-421.e5.
109. Alexander, R.K., et al., *Bmal1 integrates mitochondrial metabolism and macrophage activation.* eLife, 2020. **9**: p. e54090.
110. Lee, C.-C., et al., *Macrophage-secreted interleukin-35 regulates cancer cell plasticity to facilitate metastatic colonization.* Nature Communications, 2018. **9**(1): p. 3763.
111. Certo, M., et al., *Understanding lactate sensing and signalling.* Trends Endocrinol Metab, 2022. **33**(10): p. 722-735.

112. Liu, C., et al., *Transcriptional coactivator PGC-1alpha integrates the mammalian clock and energy metabolism.* Nature, 2007. **447**(7143): p. 477-81.
113. Odegaard, J.I., et al., *Macrophage-specific PPARγ controls alternative activation and improves insulin resistance.* Nature, 2007. **447**(7148): p. 1116-1120.
114. Daniel, B., et al., *The Nuclear Receptor PPARγ Controls Progressive Macrophage Polarization as a Ligand-Insensitive Epigenomic Ratchet of Transcriptional Memory.* Immunity, 2018. **49**(4): p. 615-626.e6.
115. Gautier, E.L., et al., *Systemic analysis of PPARγ in mouse macrophage populations reveals marked diversity in expression with critical roles in resolution of inflammation and airway immunity.* J Immunol, 2012. **189**(5): p. 2614-24.
116. Walton, Z.E., R.C. Brooks, and C.V. Dang, *mTOR Senses Intracellular pH through Lysosome Dispersion from RHEB.* Bioessays, 2019: p. e1800265.
117. Guellaen, G., et al., *RMI 12330 A, an inhibitor of adenylate cyclase in rat liver.* Biochim Biophys Acta, 1977. **484**(2): p. 465-75.
118. Hunt, N.H. and T. Evans, *RMI 12330A, an inhibitor of cyclic nucleotide phosphodiesterases and adenylate cyclase in kidney preparations.* Biochim Biophys Acta, 1980. **613**(2): p. 499-506.
119. van Rossum, D.B., et al., *Ca2+ entry mediated by store depletion, S-nitrosylation, and TRP3 channels. Comparison of coupling and function.* J Biol Chem, 2000. **275**(37): p. 28562-8.
120. O'Neill, J.S. and A.B. Reddy, *The essential role of cAMP/Ca2+ signalling in mammalian circadian timekeeping.* Biochem Soc Trans, 2012. **40**(1): p. 44-50.
121. Ni, L., et al., *Identification and Function of Acid-sensing Ion Channels in RAW 264.7 Macrophage Cells.* Curr Med Sci, 2018. **38**(3): p. 436-442.
122. Selezneva, A., A.J. Gibb, and D. Willis, *The contribution of ion channels to shaping macrophage behaviour.* Front Pharmacol, 2022. **13**: p. 970234.
123. Finger, A.M., et al., *Intercellular coupling between peripheral circadian oscillators by TGF-β signaling.* Sci Adv, 2021. **7**(30).
124. Massagué, J., *TGFb in Cancer.* Cell, 2008. **134**(2): p. 215-230.
125. Lavin, Y., et al., *Innate Immune Landscape in Early Lung Adenocarcinoma by Paired Single-Cell Analyses.* Cell, 2017. **169**(4): p. 750-765.e17.
126. Storrs, E.P., et al., *High-dimensional deconstruction of pancreatic cancer identifies tumor microenvironmental and developmental stemness features that predict survival.* NPJ Precis Oncol, 2023. **7**(1): p. 105.
127. Takahashi, J.S., *Transcriptional architecture of the mammalian circadian clock.* Nat Rev Genet, 2017. **18**(3): p. 164-179.
128. Kato, Y., et al., *Chapter Ten - DEC1/STRA13/SHARP2 and DEC2/SHARP1 Coordinate Physiological Processes, Including Circadian Rhythms in Response to Environmental Stimuli*, in *Current Topics in Developmental Biology*, R. Taneja, Editor. 2014, Academic Press. p. 339-372.
129. Sato, S., et al., *A circadian clock gene, Rev-erbalpha, modulates the inflammatory function of macrophages through the negative regulation of Ccl2 expression.* J Immunol, 2014. **192**(1): p. 407-17.
130. Billon, C., et al., *RORγ regulates the NLRP3 inflammasome.* Journal of Biological Chemistry, 2019. **294**(1): p. 10-19.
131. Geiger, S.S., et al., *Daily variation in macrophage phagocytosis is clock-independent and dispensable for cytokine production.* Immunology, 2019.
132. Committee, N.R.C., *Guide for the Care and Use of Laboratory Animals*, in *Guide for the Care and Use of Laboratory Animals*. 2011, National Academies Press (US)

133. Clausen, B.E., et al., *Conditional gene targeting in macrophages and granulocytes using LysMcre mice.* Transgenic Res, 1999. **8**(4): p. 265-77.
134. Storch, K.F., et al., *Intrinsic circadian clock of the mammalian retina: importance for retinal processing of visual information.* Cell, 2007. **130**(4): p. 730-741.
135. Trouplin, V., et al., *Bone marrow-derived macrophage production.* J Vis Exp, 2013(81): p. e50966.
136. Gonçalves, R. and D.M. Mosser, *The Isolation and Characterization of Murine Macrophages.* Current Protocols in Immunology, 2015. **111**(1): p. 14.1.1-14.1.16.
137. Ray, A. and B.N. Dittel, *Isolation of mouse peritoneal cavity cells.* J Vis Exp, 2010(35).
138. Layoun, A., M. Samba, and M.M. Santos, *Isolation of murine peritoneal macrophages to carry out gene expression analysis upon Toll-like receptors stimulation.* J Vis Exp, 2015(98): p. e52749.
139. De Jesus, A., et al., *Optimized protocol to isolate primary mouse peritoneal macrophage metabolites.* STAR Protoc, 2022. **3**(4): p. 101668.
140. Ramanathan, C., et al., *Cell Type-Specific Functions of Period Genes Revealed by Novel Adipocyte and Hepatocyte Circadian Clock Models.* PLOS Genetics, 2014. **10**(4): p. e1004244.
141. Liu, P.S., et al., *alpha-ketoglutarate orchestrates macrophage activation through metabolic and epigenetic reprogramming.* Nat Immunol, 2017. **18**(9): p. 985-994.
142. Huber, A.L., et al., *CRY2 and FBXL3 Cooperatively Degrade c-MYC.* Mol Cell, 2016. **64**(4): p. 774-789.
143. Tomayko, M.M. and C.P. Reynolds, *Determination of subcutaneous tumor size in athymic (nude) mice.* Cancer Chemother Pharmacol, 1989. **24**(3): p. 148-54.
144. Chen, S., et al., *fastp: an ultra-fast all-in-one FASTQ preprocessor.* Bioinformatics, 2018. **34**(17): p. i884-i890.
145. Patro, R., et al., *Salmon provides fast and bias-aware quantification of transcript expression.* Nat Methods, 2017. **14**(4): p. 417-419.
146. Soneson, C., M.I. Love, and M.D. Robinson, *Differential analyses for RNA-seq: transcript-level estimates improve gene-level inferences.* F1000Res, 2015. **4**: p. 1521.
147. Ritchie, M.E., et al., *limma powers differential expression analyses for RNA-sequencing and microarray studies.* Nucleic Acids Res, 2015. **43**(7): p. e47.
148. Dai, M., et al., *Evolving gene/transcript definitions significantly alter the interpretation of GeneChip data.* Nucleic Acids Res, 2005. **33**(20): p. e175.
149. Butler, A., et al., *Integrating single-cell transcriptomic data across different conditions, technologies, and species.* Nature Biotechnology, 2018. **36**(5): p. 411-420.
150. Becht, E., et al., *Dimensionality reduction for visualizing single-cell data using UMAP.* Nature Biotechnology, 2019. **37**(1): p. 38-44.
151. Smyth, G.K., *limma: Linear Models for Microarray Data*, in *Bioinformatics and Computational Biology Solutions Using R and Bioconductor*, R. Gentleman, et al., Editors. 2005, Springer New York: New York, NY. p. 397-420.

Fig 1

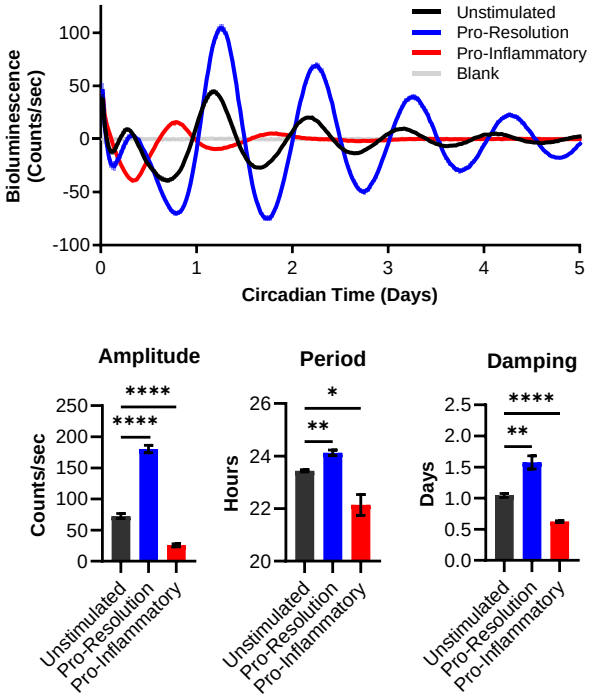

Fig 2

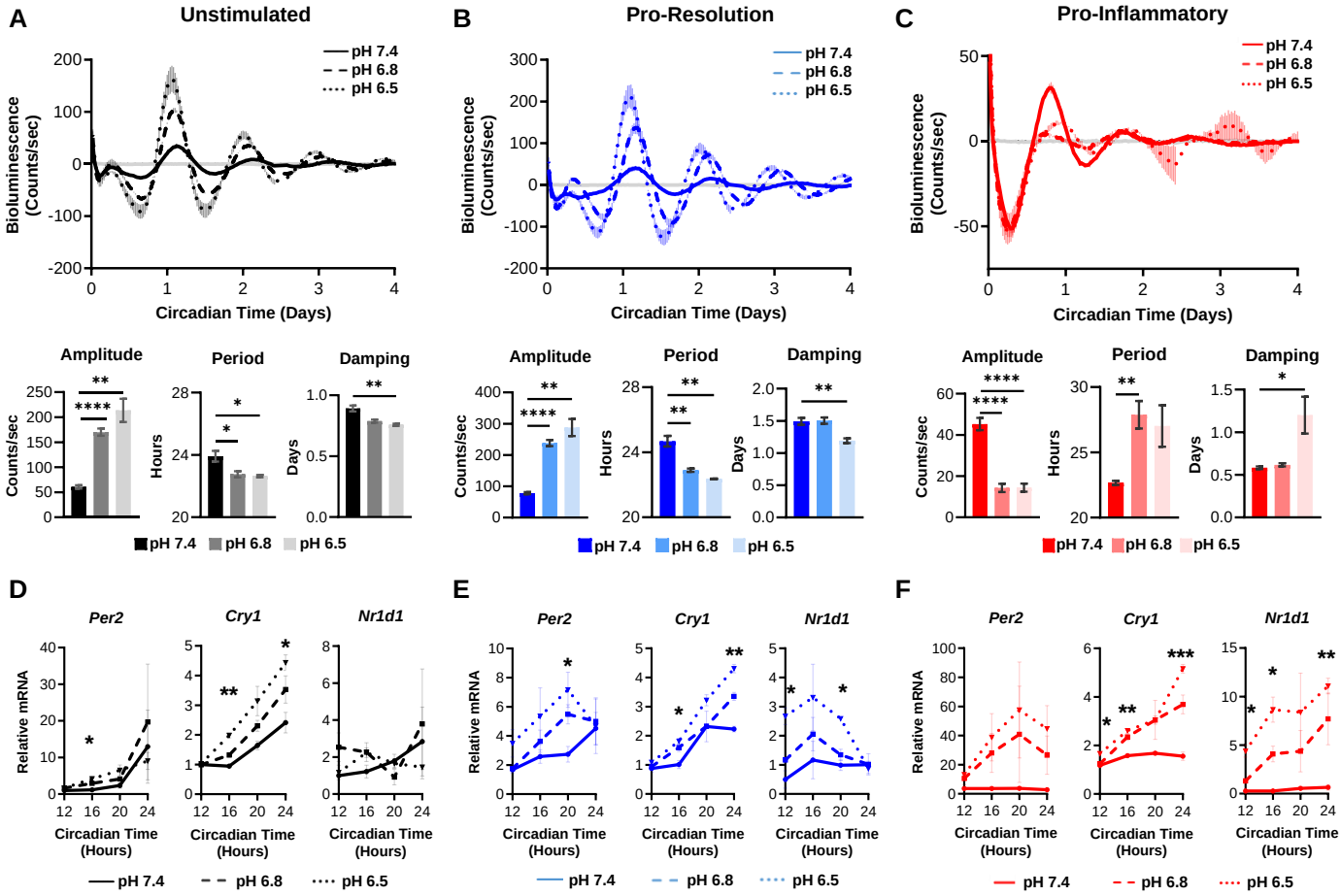

Fig 3

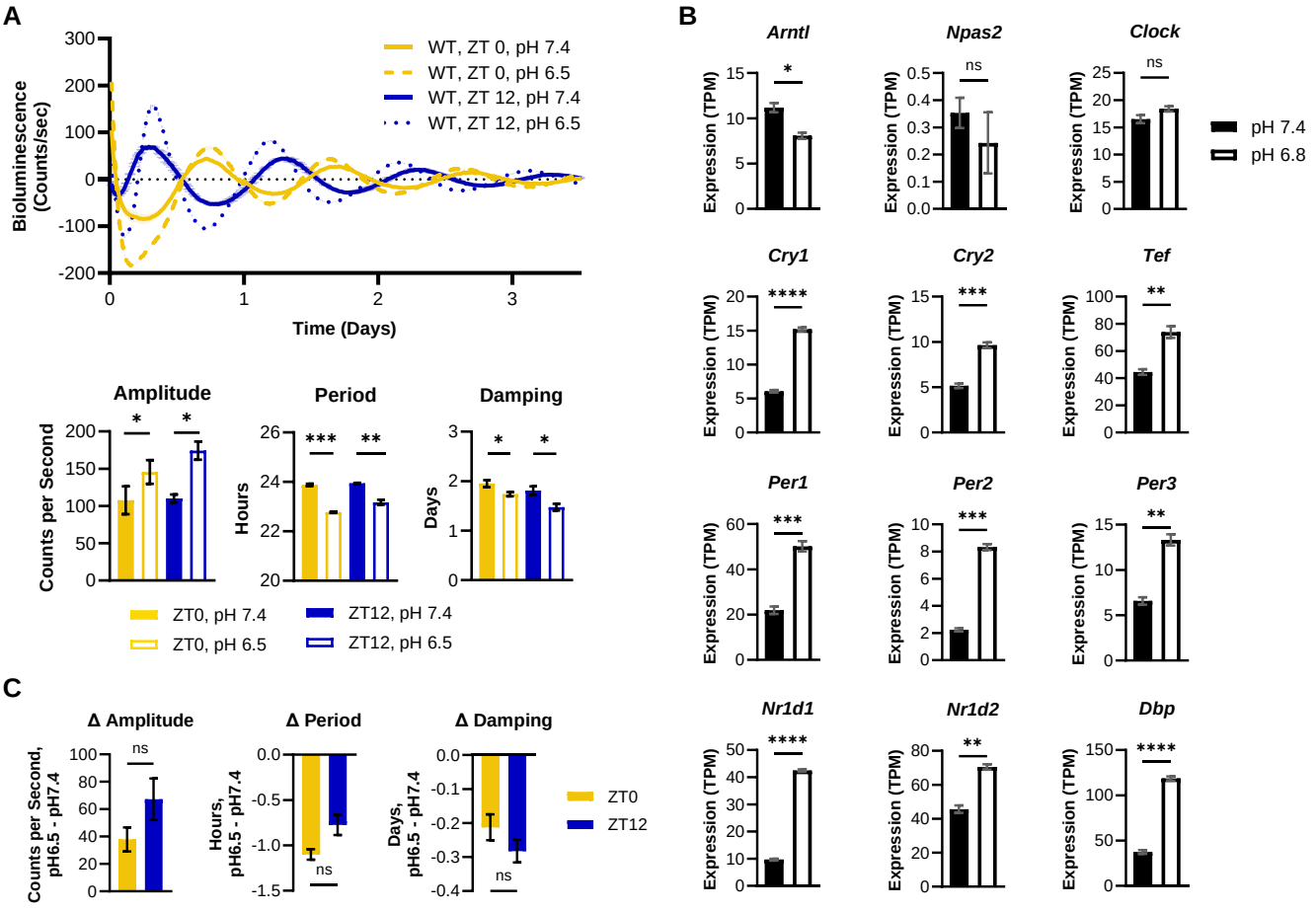

Fig 4

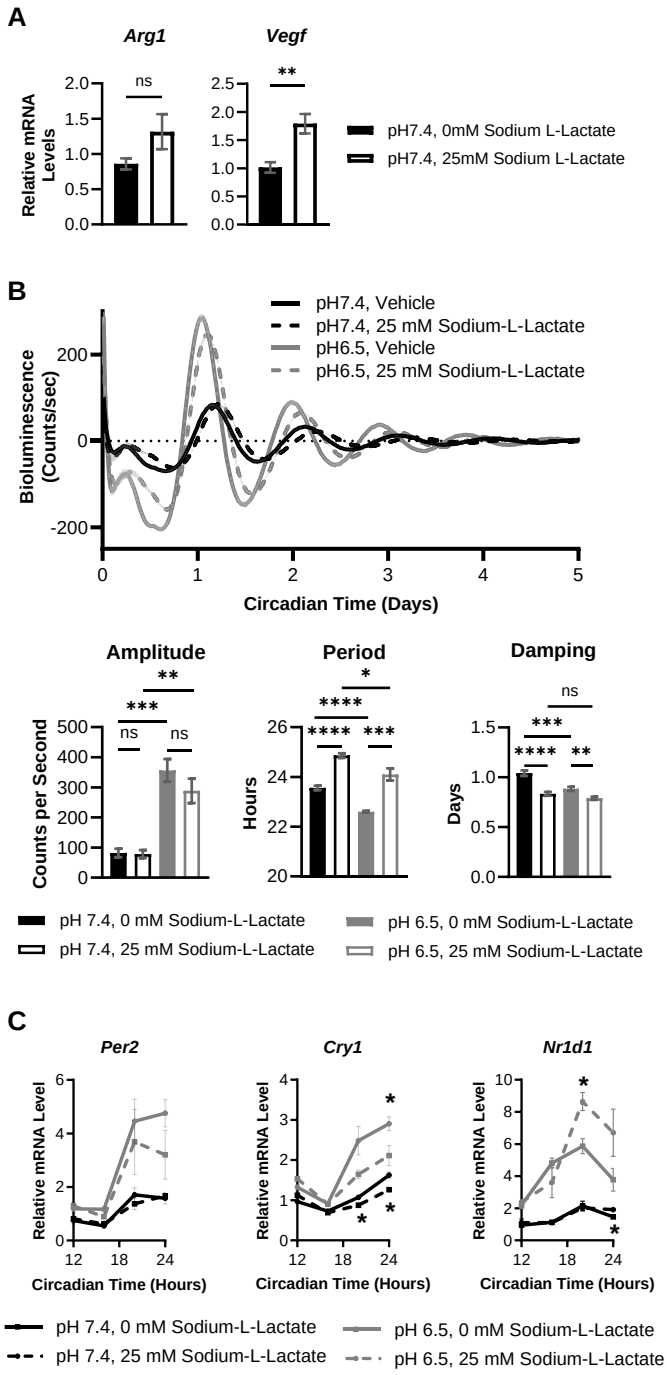

Fig 5

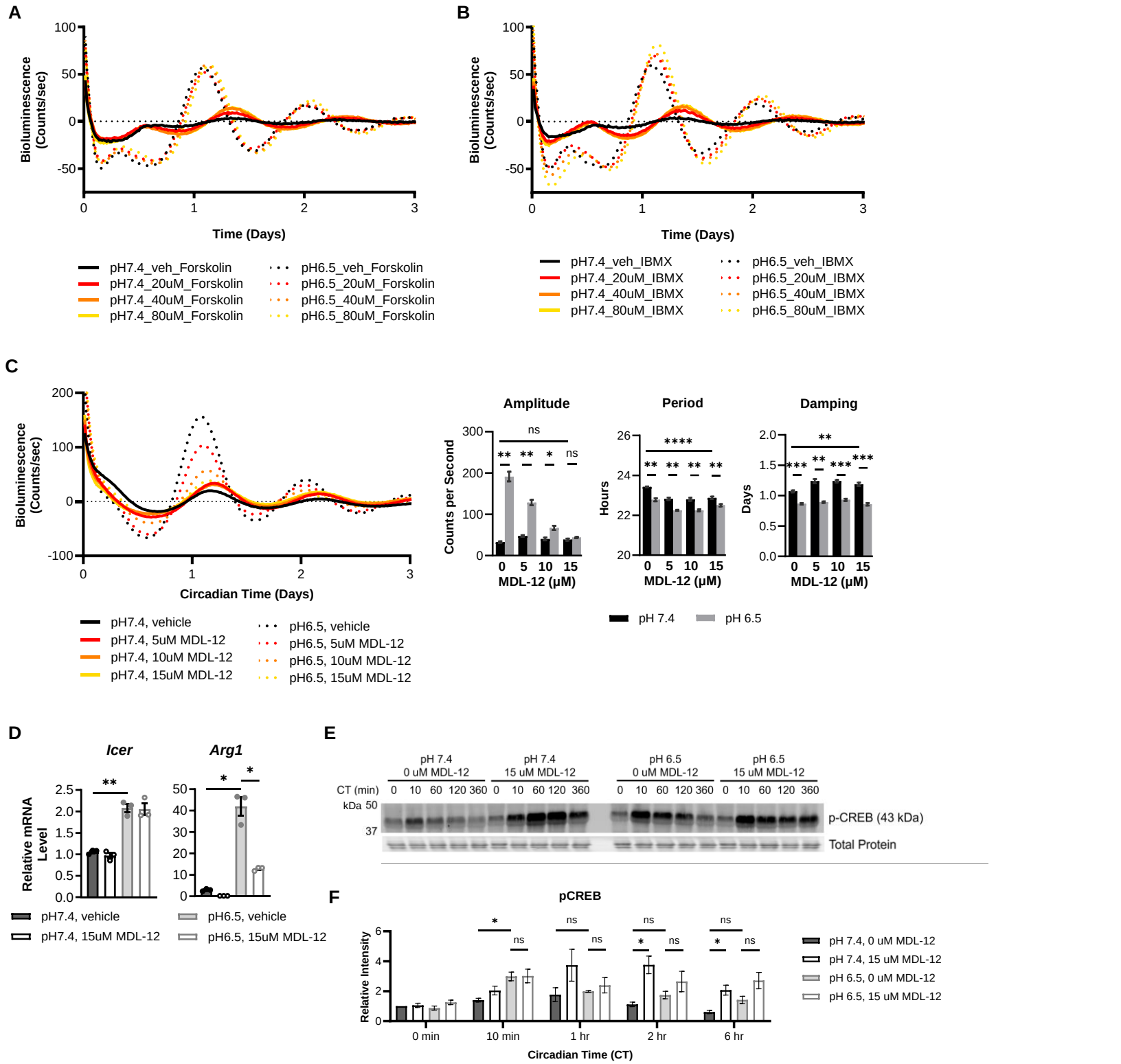

Fig 6

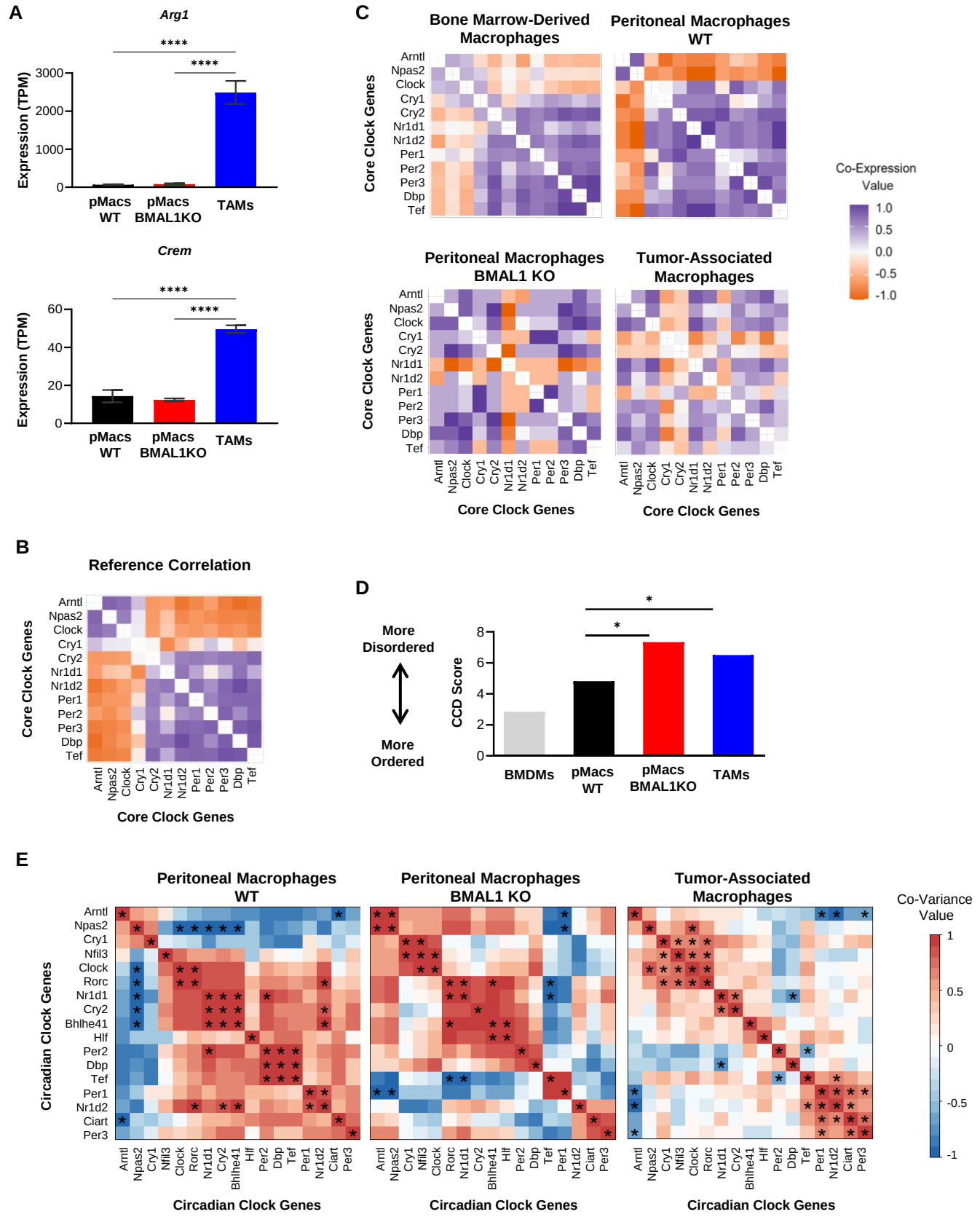

Fig 7

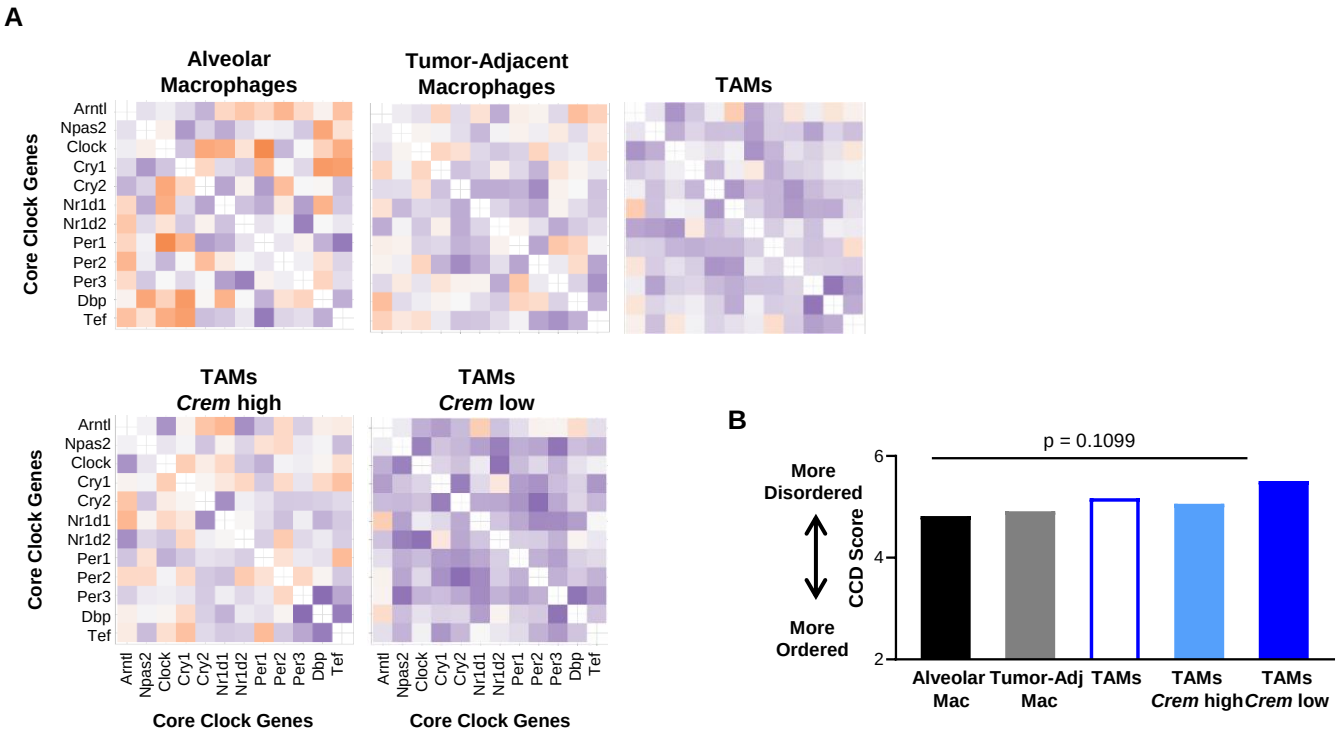

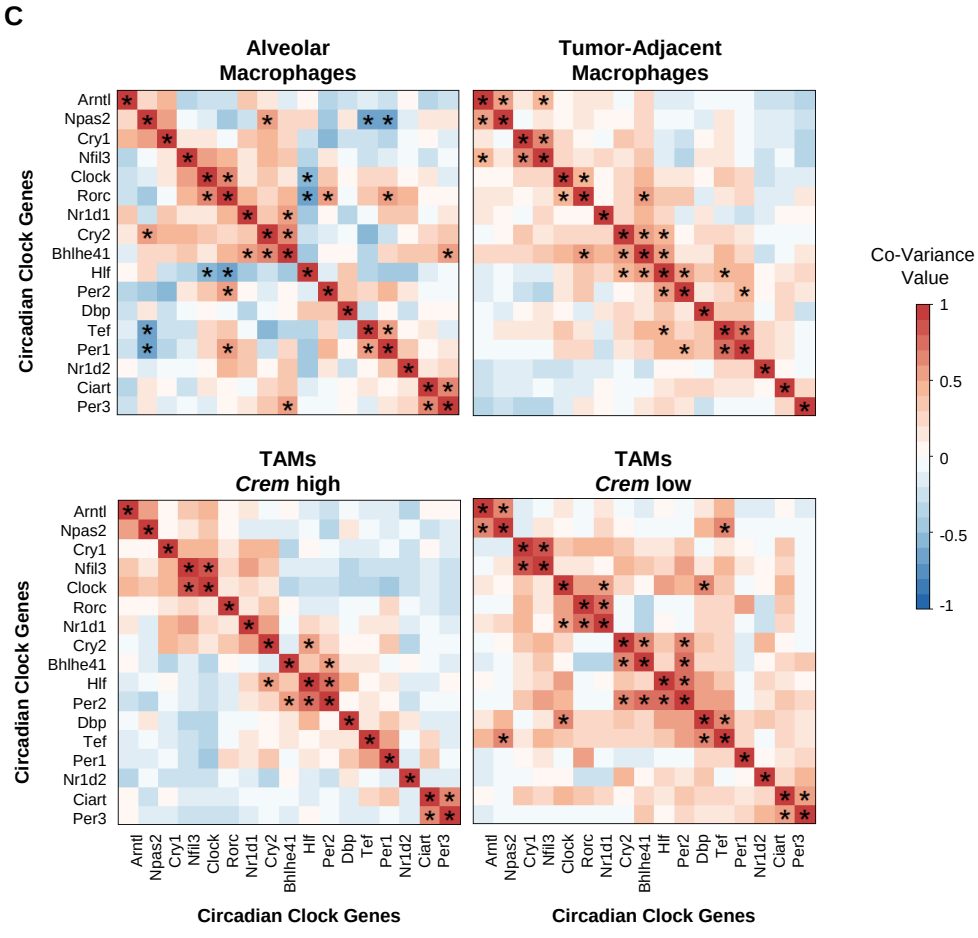

Fig 8

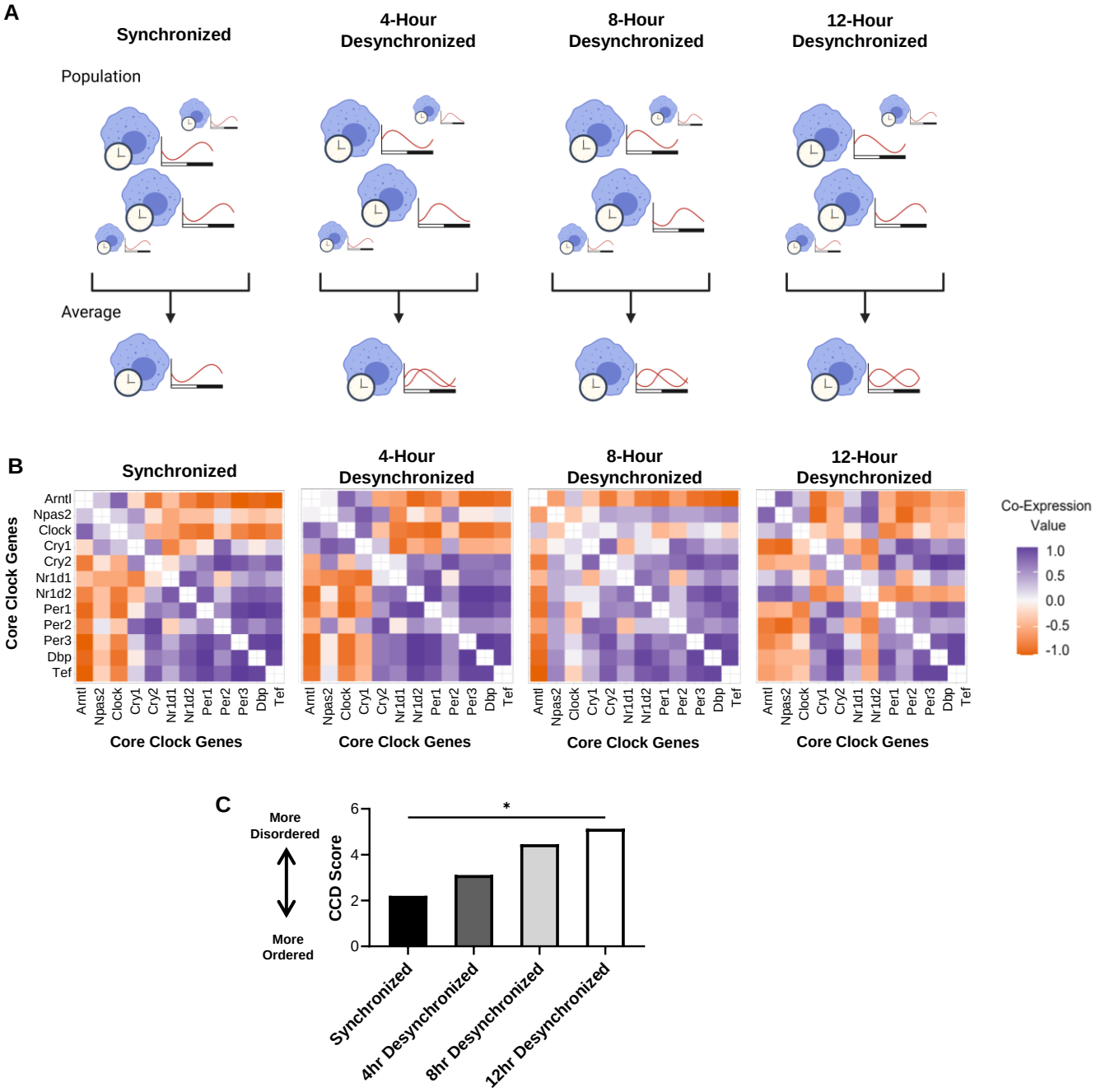

Fig 9

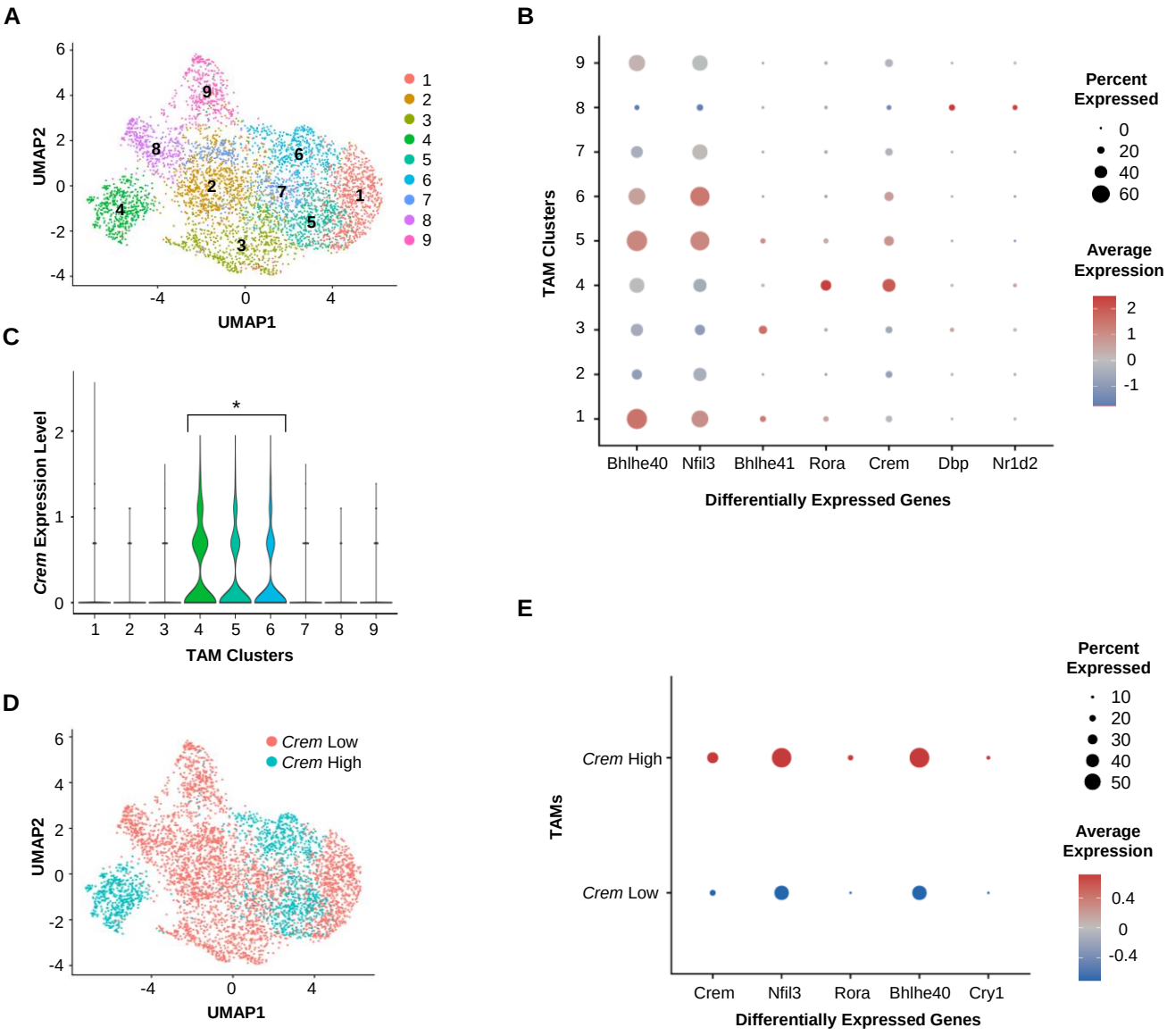

Fig 10